MAX-PLANCK-INSTITUT FÜR PHYSIK
WERNER-HEISENBERG-INSTITUT

MPI-PhE/96-19
October 1996

BEAUTY HADRON PROPERTIES [1]

Stefan Schael
Max-Planck Institut für Physik (Werner Heisenberg Institut)
Föhringer Ring 6, D-80805 München, Germany

Abstract

The data taking for LEP I was finished. This summer nearly all LEP experiments presented their final numbers for B hadron lifetimes and masses, for the production rates and properties of excited beauty states, for the measurement of $B_d^0\bar{B}_d^0$ oscillations and for the search for $B_s^0\bar{B}_s^0$ oscillations. Impressive new results on B_s^0 and Λ_b lifetimes and masses were presented by CDF. The experimental situation is summarised in this article.

[1] Talk, presented at the XVI International Conference on Physics in Collision, Mexico City, Mexico, June 19-21, 1996.

BEAUTY HADRON PROPERTIES [1]

Stefan Schael
Max-Planck Institut für Physik (Werner Heisenberg Institut)
Föhringer Ring 6, D-80805 München, Germany

Abstract

The data taking for LEP I was finished. This summer nearly all LEP experiments presented their final numbers for B hadron lifetimes and masses, for the production rates and properties of excited beauty states, for the measurement of $B_d^0\bar{B}_d^0$ oscillations and for the search for $B_s^0\bar{B}_s^0$ oscillations. Impressive new results on B_s^0 and Λ_b lifetimes and masses were presented by CDF. The experimental situation is summarised in this article.

[1] Talk, presented at the XVI International Conference on Physics in Collision, Mexico City, Mexico, June 19-21, 1996.

1 B Hadron Lifetimes and Masses

Heavy quark decays can be described in the framework of the spectator model (see Fig. 1). The long B lifetime is a consequence of the small Kobayashi-Maskawa coupling between b and c quarks that neutralises the effect of the large mass m_b in the Fermi decay of the b quark. While one expects $\tau(D^0) = \tau(D^+)$ in

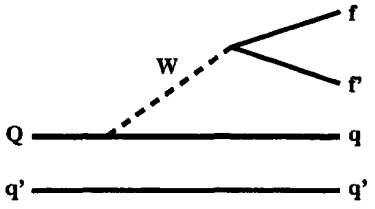

Figure 1: Heavy quark decay in the spectator model.

the framework of this simple model for the charm sector, the experimental value is: $\tau(D^+)/\tau(D^0) = 2.55 \pm 0.04$ [2] in agreement with detailed calculations [3]. For the beauty sector recent calculations based on Heavy Quark Effective Theory (HQET [1]) lead to the following predictions (which have a few percent accuracy) [4]:

$$\begin{aligned} \tau(B^+)/\tau(B^0) &= 1.0 + 0.05\left(\frac{f_B}{200MeV}\right)^2 \\ \tau(B_s^0)/\tau(B^0) &= 1.0 \\ \tau(\Lambda_b)/\tau(B^0) &= 0.9 \end{aligned}$$

where f_B is the B decay constant. Thus the lifetimes should follow the pattern:

$$\tau(B^+) > \tau(B_d^0) \approx \tau(B_s^0) > \tau(\Lambda_b)$$

The B lifetime measurements are important inputs for the calculation of the CKM-Matrix element V_{cb} from the semileptonic branching ratio and for the study of $B^0\bar{B}^0$ oscillations and CP violation in the beauty system. From the experimental point of view a precise knowledge of the B lifetime is needed to calibrate b-tagging algorithms for the measurement of $R_b = \Gamma(Z \to b\bar{b})/\Gamma(Z \to q\bar{q})$ or for the Higgs search in the decay mode $H \to b\bar{b}$.

1.1 Inclusive B lifetime measurements

The classical method to determine the inclusive B lifetime is based on the identification of leptons from semileptonic B decays. From the measurement of the

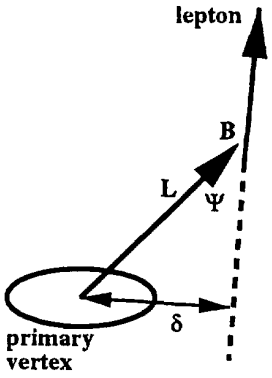

Figure 2: Impact parameter definition.

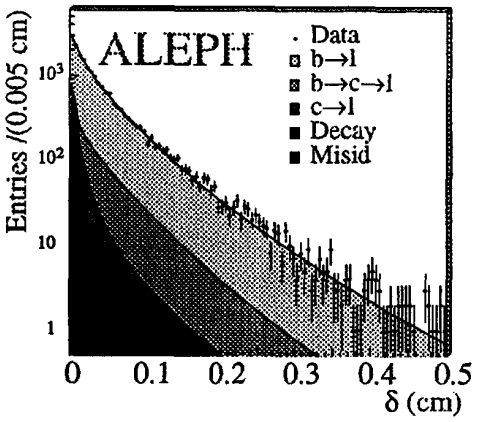

Figure 3: Lepton impact parameter distribution from ALEPH.

impact parameter (δ) of the leptons (see Fig. 2) which is defined as

$$\delta = \gamma \cdot \beta \cdot c \cdot \tau_B \cdot |\sin\Theta| \cdot \sin\Psi \tag{1}$$

the B lifetime is extracted. This technique was developed at PEP and PETRA and is nowadays used for precision measurements at LEP and SLC. It has the advantage that it is rather insensitive to the B hadron boost, since $\sin\Psi \propto \gamma^{-1}$ and therefore $\delta \sim c \cdot \tau_B$. Nevertheless Monte Carlo studies are needed to determine the exact relation between lifetime and impact parameter. The typical flight lenght for a B hadron produced in e^+e^- annihilation at 91 GeV centre of mass energy is $\approx$ 2.6 mm. The vertex detector resolution for the LEP experiments in the $r\phi$ plane are $\sigma_{r\phi} = 12\mu m$ and $\sigma_z = (12 - 22)\ \mu m$ [5] along the beam direction. The primary vertex position is reconstructed with a precision of $\sigma_x \approx 50\ \mu m$, $\sigma_y \approx 10\ \mu m$ and $\sigma_z \approx 60\ \mu m$. The position in the x, y plane is determined from a sample of typically hundred events, while the z position has to be calculated on an event-by-event basis. The final impact parameter resolution at LEP is $\sigma_\delta = 70\ \mu m$.

The lepton impact parameter distribution as measured by the ALEPH experiment is shown in Fig. 3 based on a data sample of 1.5 million hadronic events recorded in the years 1991 through 1993. Semileptonic B decays are selected by requiring the presence of a lepton candidate with a momentum p greater than 3 GeV/c and a transverse momentum p_t, relative to the associated jet axis, greater than 1 GeV/c. This rejects most of the leptons from semileptonic charm decays and most of the electrons from photon conversions. The fit of the three-dimensional impact parameter distribution yields an average B hadron lifetime of $1.533 \pm 0.013(stat.) \pm 0.022(sys.)$ ps [8].

Another technique which leads to high precision measurements of the average B lifetime is the inclusive reconstruction of secondary vertices. The DELPHI experiment is able to reconstruct 23000 Vertices from a data sample of 1.5 million hadronic Z events. The decay length resolution for these vertices is $(301 \pm 24)\mu m$. They have been selected to have an invariant mass of larger than 1.7 GeV/c^2, to contain more than 4 charged tracks and to be separated from the primary vertex by more than 1.5 mm. The b purity of this sample is $(93.5 \pm 0.3)\%$ according to Monte Carlo simulation. The decay length distribution is shown in Fig. 4. The B signal was parametrised by a single exponential, exp(-L/A), whose slope A was a linear function of the B hadron lifetime. The boost of the B had to be taken from the Monte Carlo simulation, since $L = \gamma\beta c\tau_B$. The average B hadron lifetime is measured to be $\tau_B = 1.582 \pm 0.011(stat.) \pm 0.027(sys.)$ ps [10].

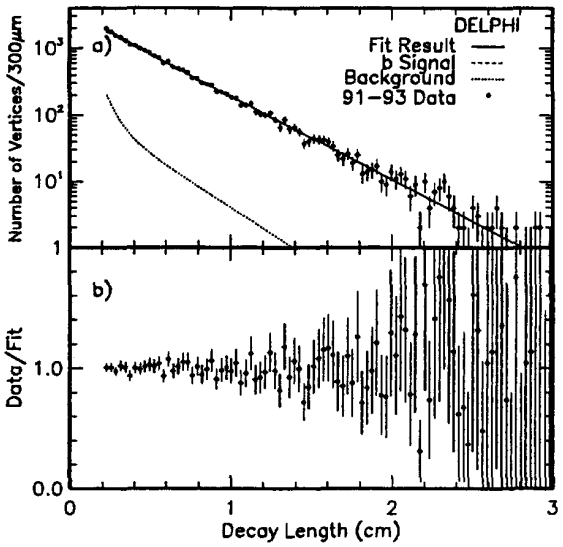

Figure 4: The decay length distribution of secondary vertices as reconstructed by the DELPHI experiment in 1.5 million Z decays.

A similar analysis was performed by the SLD experiment. The excellent vertex detector, which is much closer to the interaction point than at the LEP experiments, leads to a much higher efficiency for the inclusive reconstruction of B vertices. SLD measures the decay length distribution with 5000 vertices reconstructed from only 50000 hadronic Z decays.

The results of the inclusive B lifetime measurements are summarised in Fig. 5. In the average value, common systematic errors from the b- and c-fragmentation function, from b- and c-decay models, from the semileptonic branching-ratios ($BR(B \to l)$, $BR(B \to c \to l)$ and $BR(c \to l)$), from the c hadron lifetime and

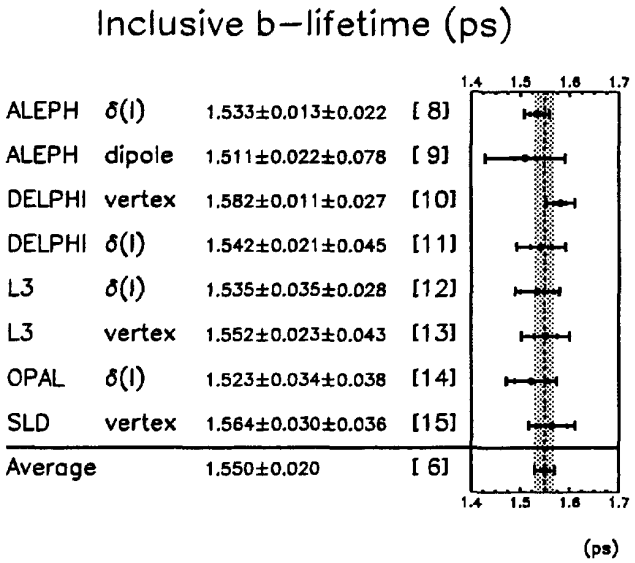

Figure 5: Measurements of the average B hadron lifetime.

from the B charged track multiplicity are taken into account [6]. Following the recipe described by R. Forty [7], the relative errors σ_i/τ_i are used as weights to compute lifetime averages throughout this paper.

Nearly all analysis are limited by their systematical errors. The dominant sources are the uncertainties in the shape of the lepton spectrum for the $b \to c \to l$ process and in the modelling of the b-fragmentation function. The average B hadron lifetime measured from 1986 until 1996 is shown in Fig. 6. Although the measurement has became rather stable since 1994, the plot makes it difficult to believe that the measurements of the four LEP experiments are really independent.

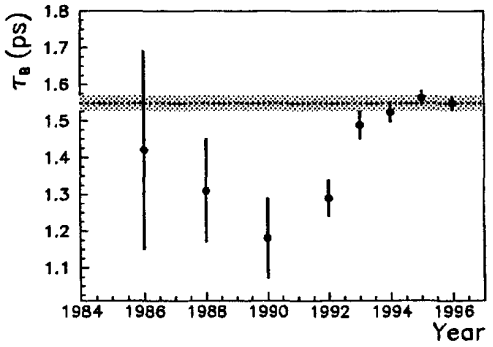

Figure 6: The average B hadron lifetime measured from 1986 to 1996.

1.2 Exclusive B lifetime measurements and B hadron masses

Semileptonic B decays have also been used for the measurement of exclusive B lifetimes (Fig. 7).

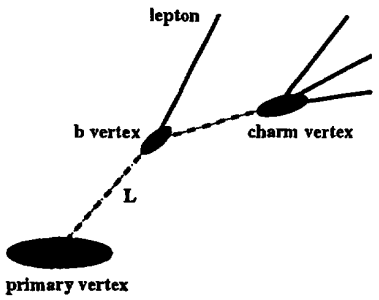

Figure 7: Schematic view of a semileptonic B decay.

It is straight forward to reconstruct the B decay vertex after the lepton is identified and the charm hadron (X_c) is reconstructed in one of its known decay modes. The typical decay length resolution is $\sigma_L \approx 300\mu m$. To measure the lifetime also the B hadron energy needs to be determined ($\tau_B = L \cdot M_B/P_B$). Depending on the different experimental setups various techniques have been developed for this purpose. Experiments with good hermiticity try first to estimate the energy of the missing neutrino from the total visible energy in the hemisphere. Corrections are than determined from Monte Carlo models to estimate the B hadron energy either from the (X_c, l)- or from the (X_c, l, ν_l)-system. The best resolution has been obtained by two dimensional correction functions based on $(P(X_c l), M(X_c l))$. In general the resolution is in the range $\sigma_{P_b}/P_b \approx 10-15\%$.

The following decay modes have been reconstructed by the various experiments:

$$B_d^0 \to D^{*-} l^+ \nu_l X \qquad B_u^+ \to \bar{D}^0 l^+ \nu_l X \qquad \Xi_b^- \to \Xi_c^0 l^- \nu_l X$$
$$B_s^0 \to D_s^- l^+ \nu_l X \qquad \Lambda_b \to \Lambda_c^+ l^- \nu_l X$$

Charge conjugation is implicitly assumed throughout this paper. Most of these analyses are limited by statistics due to the small charm branching-ratios to the experimental accessible decay channels. DELPHI presented this year a new measurement of the B_d^0 lifetime based on a semi-inclusive reconstruction of the $D^{*+} \to D^0\pi^+$ decay [21]. This approach has a higher statistical power than previous analyses. The D^{*+} signal obtained together with the proper time distribution for the data taking period 1991 till 1993 and 1994 is shown in Fig. 8. The data set is divided in two periods due to the vertex detector upgrade in the 1993/94

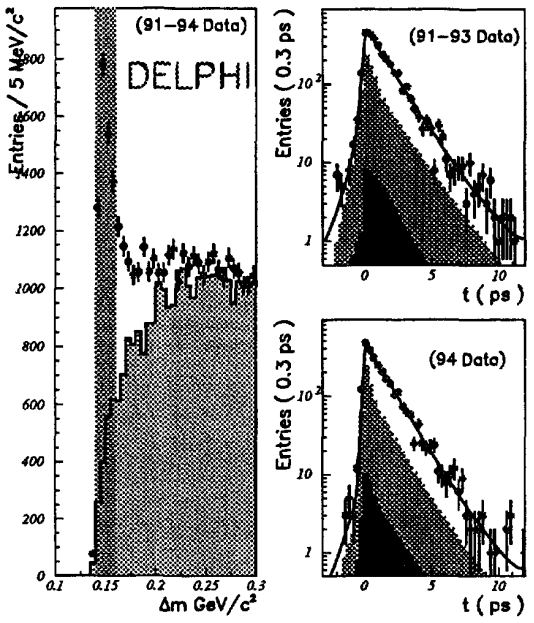

Figure 8: B_d^0 lifetime measurement by DELPHI using the $B_d^0 \to D^{*-} l^+ \nu_l X$ decay mode. The left plot shows the signal for the $D^{*-} \to D^0 \pi^-$ decay and the right upper and lower plots the proper time distribution for the 1991 till 1993 and 1994 data taking periods, respectively.

shutdown. From a sample of 4130 reconstructed decay vertices a B^0 lifetime of $\tau(B^0) = (1.500^{+0.038}_{-0.037} \pm 0.041)\ ps$ [21] is measured.

DELPHI [20] and SLD [24] have measured B_d^0 and B_s^0 lifetimes using inclusive reconstructed secondary vertices for which the charge of the vertex indicates the B charge. Care must be taken to exclude events with tracks that are ambiguous between production and decay vertex. DELPHI finds 1817 B hadron vertices from 1.4 million hadronic Z decays. The B purity was estimated to be (99.1 ± 0.3) %. According to the Monte Carlo simulation 83% (70%) of the events measured as neutral (charged) came from neutral (charged) B's. With assumptions on the B_s^0 and Λ_b production fractions and lifetimes, the B_d^0 lifetime can be determined from the neutral B lifetime.

Fully reconstructed B decays have been used by ALEPH [16] and CDF [17] to measure B lifetimes. While the ALEPH result is obtained by adding various decay channels, CDF is able to perform such analysis based only on $B \to J/\Psi K$ decays modes. Although these analysis are currently limited by statistics they have the advantage that they are independent of Monte Carlo models to determine the B hadron boost.

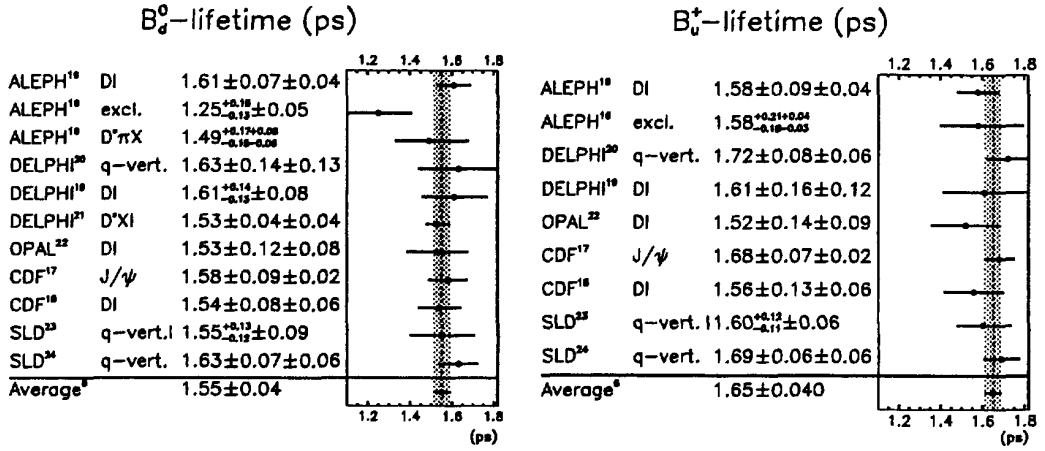

Figure 9: Summary of the B_d^0 and B^+ lifetime measurements.

The measurements of the B_d^0 and B^+ lifetimes are summarised on Fig. 9. For the weighted mean the background composition (includes D^{**} branching ratio uncertainties), the B hadron momentum estimation, the lifetimes of B_s and B baryons, and the production fraction of B_s ($f_s = 0.12 \pm 0.04$) and of B baryons ($f_{\Lambda_b} = 0.08 \pm 0.04$) where considered as correlated systematic uncertainties.

Compared to SLC and the LEP experiments CDF has the advantage of the large $b\bar{b}$ production cross section and presented this summer impressive new measurements [29] [35]. They where able to reconstruct 32 ± 6 $B_s \to J/\Psi\Phi$ decays (see Fig. 10) and 197 ± 25 right sign $\Lambda_c l$ combinations from the decay chain: $\Lambda_b \to \Lambda_c l\nu, \Lambda_c \to pK^-\pi^+$ (see Fig. 11). Using their full statistics from the 1992 till 1995 data, corresponding to 115 pb^{-1} they also observed $\Lambda_b \to \Lambda J/\Psi$ decays, which had been expected for a long time [25]. From a signal of 38 events with an estimated background of 18.3 events the Λ_b mass is measured to be: $M(\Lambda_b) = (5623 \pm 5 \pm 4)\ MeV/c^2$.

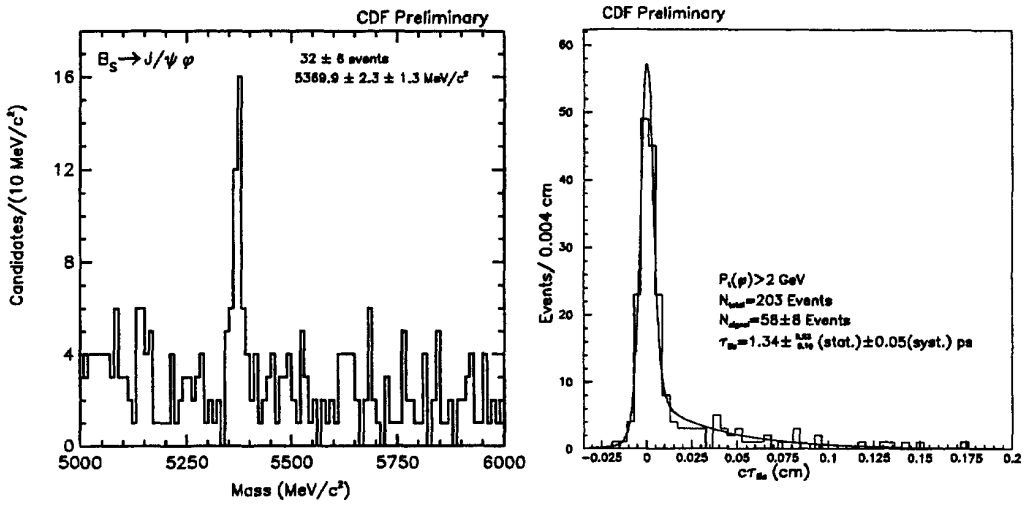

Figure 10: $B_s \to J/\Psi\Phi$ decays as reconstructed by CDF. The left plot shows the invariant mass distribution while the right plot shows the decay length distribution in the signal region.

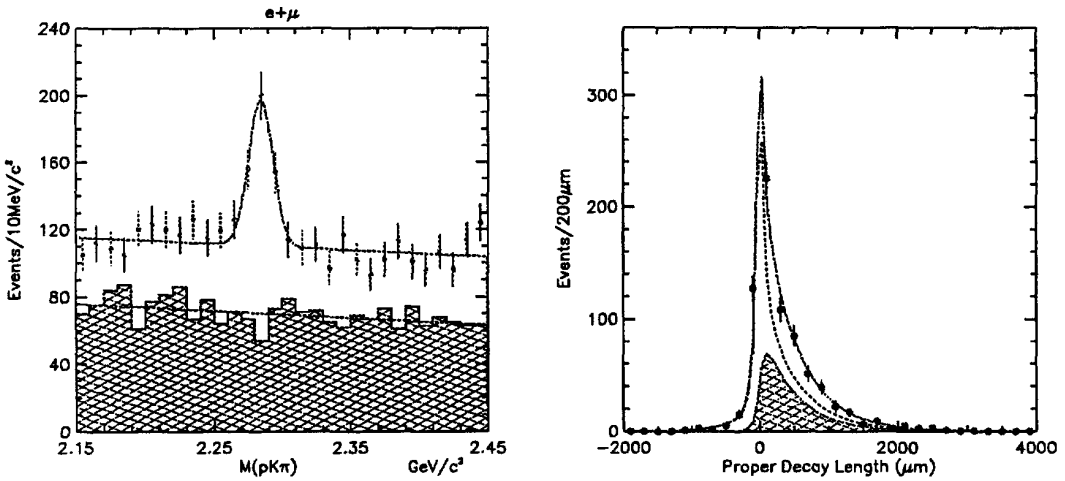

Figure 11: $\Lambda_c l$ correlations as observed by CDF. The left plot shows the Λ_c signal for the right charge $\Lambda_c l$ combinations (dots) and the wrong charge combinations (shaded histogram). The right plot shows the proper decay length distribution in the Λ_c signal region. The shaded area is the signal distribution while the dashed line shows the background contribution.

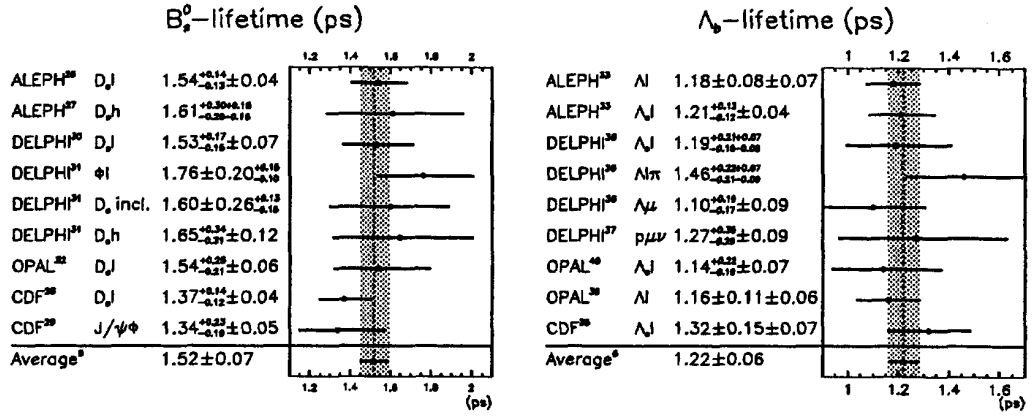

Figure 12: Summary of the B_s^0 and Λ_b lifetime measurements.

The B_s and Λ_b lifetime measurements are summarised on Fig. 12. As correlated systematic uncertainties for the weighted mean of the B_s lifetime, the average B lifetime used in the background estimation, the B_s decay multipiclity and the B_s branching ratios were considered. For the average of the Λ_b lifetime, the systematic error due to the Λ_b fragmentation function, the Λ_b polarisation and Λ_b decay models where considered to be correlated between the experiments.

No new measurements of B_d^0 mass ($M(B_d^0) = (5279.2 \pm 1.8)\ MeV/c^2$) [2] and of the B^+ mass ($M(B^+) = (5278.9 \pm 1.8)\ MeV/c^2$) [2] were presented this summer. The measurements of the B_s- and Λ_b-mass, which are dominated by the CDF results, are given on Fig. 13. All B hadron mass measurements have reached now a precision of better than 0.11%.

A new measurement of the Ξ_b^- lifetime was presented this summer by ALEPH [34] using the decay mode $\Xi_b^- \to \Xi_c^0 l^- \nu_l X$, $\Xi_c^0 \to \Xi^- X$. 30 right sign Ξl and

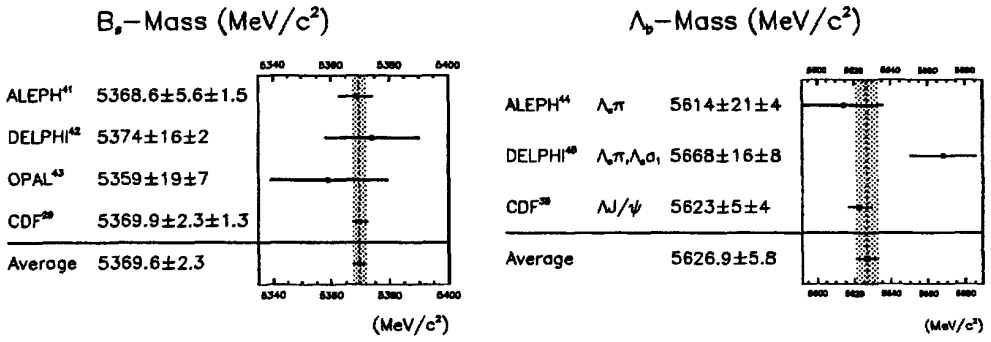

Figure 13: Summary of the B_s^0 and Λ_b mass measurements.

3 wrong sign Ξl combinations where reconstructed from 3.93 million Z decays in the decay mode $\Xi^- \to \Lambda\pi^-$. The estimated background is 4.2 ± 2.4 events. A Ξ_b lifetime of $\tau_{\Xi_b} = (1.35^{+0.37}_{-0.28} \pm 0.17)$ *ps* is obtained from the lepton impact parameter distribution as shown in Fig.14. A similar measurement performed by

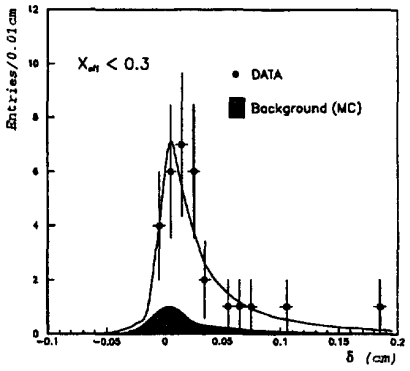

Figure 14: Impact parameter distribution of lepton candidates from $\Xi_b^- \to \Xi_c^0 l^- \nu_l X$ decays as measured by ALEPH.

DELPHI [38] yields $\tau_{\Xi_b} = (1.5^{+0.7}_{-0.4} \pm 0.3)$ *ps*. Since the total error for the world average of $\tau(\Xi_b) = (1.39^{+0.36}_{-0.27})$ *ps* is still large it can not support the hypothesis, indicated by the Λ_b lifetime, that the average B baryon lifetime is shorter than the B meson lifetime.

1.3 B_c: A first candidate

This summer a first B_c candidate has been shown by ALEPH [46]. It is reconstructed in the decay mode $B_c \to J/\Psi\mu\nu_\mu$. The theoretical predictions for the B_c mass are $M(B_c) = (6.25 \pm 0.05)\ GeV/c^2$ and for the B_c lifetime in the range $\tau(B_c) = (0.4 - 1.4)$ *ps*. In 1 million hadronic Z decays one expects 100-700 B_c mesons to be produced. The branching-ratio in the quoted decay channel is calculated to be $BR(B_c \to J/\Psi l\nu) = (1 - 3)\ \%$.

The J/Ψ is reconstructed in the decay channel $J/\Psi \to e^+e^-$ with a mass of $M(e^+e^-) = (3.102 \pm 0.014)\ GeV/c^2$, in good agreement with the nominal J/Ψ mass [2]. The probability for the track which is identified as a muon to be a pion or kaon is $\mathcal{P}(\mu) = \pi$: 10^{-4} and $\mathcal{P}(\mu) = K$: 10^{-5} respectively. A view of the primary vertex region from the ALEPH event display is shown in Fig. 15. The $(J/\Psi\mu)$ vertex is clearly separated from the primary vertex. The reconstructed decay length is (2.546 ± 0.077) *mm*. Since the mass of the $(J/\Psi\mu)$ combination is with $(5.640 \pm 0.015)\ GeV/c^2$ larger than the B_s mass it can be excluded that this

is a decay from one of the known B meson states with one track being misidentified. From Monte Carlo simulations it could been shown that the probability that this B_c candidate is a decay chain $B^{\pm} \rightarrow J/\Psi K^{\pm}, K^{\pm} \rightarrow \mu\nu_{\mu}$ is less than 10^{-5}. Also using Monte Carlo simulations the background from B_{ud} and B_s decays has been estimated to be less than $2 \cdot 10^{-3}$.

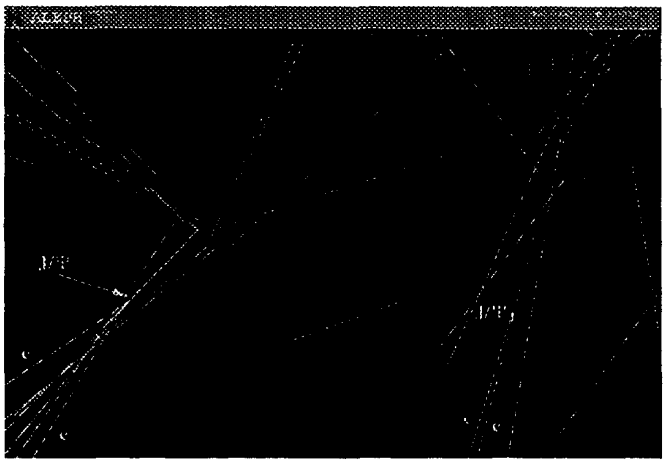

Figure 15: The primary vertex region of the B_c event candidate. A clear three jet structure, as expected for a B_c event is observed. The B_c flight path is indicated by the dashed line.

Using the missing energy in the hemisphere and the B_c flight direction as measured by the vector pointing from the primary vertex to the $(J/\Psi\mu)$ vertex the momentum vector of the neutrino can be reconstructed. The obtained B_c mass is: $M(B_c) = (5.96^{+0.25}_{-0.19})\ GeV/c^2$ and the lifetime of this candidate is $\tau(B_c) = (1.77 \pm 0.17)\ ps$.

1.4 Summary of the B lifetime measurements

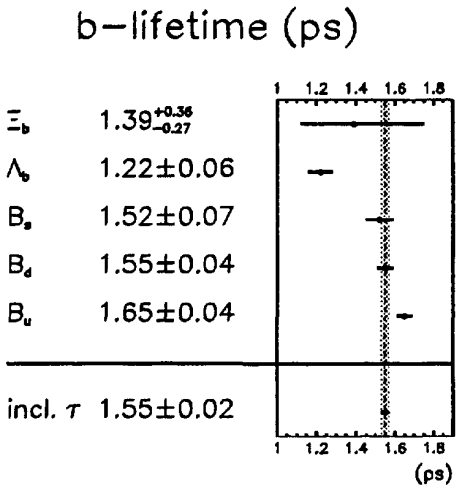

Figure 16: The B lifetime measurements.

The experimental situation for the B lifetime measurements is summarised in Fig. 16. The Λ_b lifetime is significantly shorter than the average B meson lifetime and even shorter than expected. The individual lifetime measurements have reached a precision of up to 2%. The lifetime ratio $\tau(B^+)/\tau(B^0)$ is within the errors compatible with unity (see Fig. 17) and in agreement with the theoretical expectations.

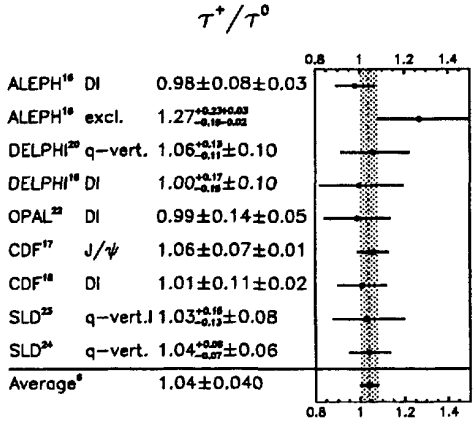

Figure 17: Measurements of $\tau(B^+)/\tau(B^0)$.

2 Excited Beauty States

The low lying $B(1S)$ states, B and B^*, are well established [2]. Due to the small mass splitting between B^* and B mesons only electromagnetic decays of the B^* to $B\gamma$ are allowed. At LEP an inclusive reconstruction of B^* states is performed by association of a converted photon to a jet selected to have the B meson momentum and direction. The B^* mass and production rate is obtained. Replacing the photon by a charged track the technique is extended to a search of B^{**} states.

The fraction of b quarks forming a B^{**} state is of great interest since their expected decay modes into $B^{(*)}\pi^{\pm}$ can be used to identify the flavour of the b quark at the production time (see Fig. 18). Recently a method based on

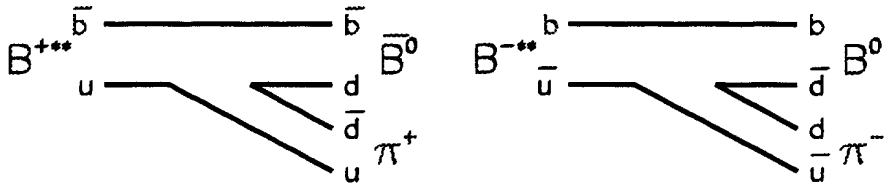

Figure 18: Diagram for the $B^{**} \to B^{(*)}\pi$ decay.

this idea has been proposed to measure CP-violation in the decay of the neutral B meson [47]. Due to this proposal much effort was made to predict the properties of the B^{**} states based on extrapolations from the K^{**} and D^{**} sectors [48]. They are summarised in table 1. The fine structure of the L = 1 system is dominated by whether the sum $L + S_q = j$ corresponds to $j = 1/2$ or $j = 3/2$.

The relative production rate of B^* mesons is expected to be $N_{B^*}/(N_B +$

	$q = u, d$		
State (J_j^P)	Mass (GeV/c^2)	Width (GeV)	Decay mode
$1^+_{3/2}$	5.76	0.020	$(B^*\pi)_{l=2}$
$0^+_{1/2}$	≈ 5.65	broad	$(B\pi)_{l=0}$
$1^+_{1/2}$	≈ 5.65	broad	$(B^*\pi)_{l=0}$
$2^+_{3/2}$	5.77	0.024	$(B^*\pi)_{l=2}$, $(B\pi)_{l=2}$

Table 1: Expected properties of L = 1 $b\bar{q}$ states.

N_{B^*}) = 0.75 from a simple spin counting picture [2]. The maximum energy of the photon from B^* decays is 0.8 GeV, while the mean energy is only $< E_\gamma >= 0.3$ GeV. Therefore instead of using the electro-magnetic calorimeter, which for a LEP experiment is designed to measure efficiently electro-magnetic showers with energies above 1 GeV and is hence limited in this low energy range in resolution and efficiency, the tracking system is used to reconstruct and identify converted photons.

2.1 Selection and Reconstruction of B hadrons

B hadrons are tagged using algorithm described for example in Ref. [49], in which the impact parameters of charged tracks are used to select long lived particles.

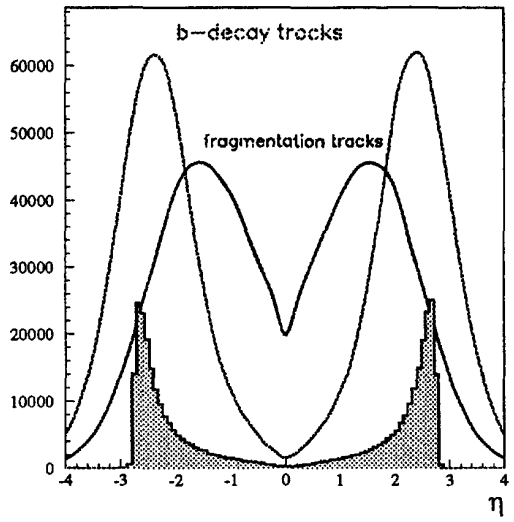

Figure 19: Rapidity distribution according to the JETSET Monte Carlo model measured relative to the thrust axis in $Z \rightarrow b\bar{b}$ events. The shaded area shows the distribution for the B hadrons.

For charged tracks two criteria are available to decide whether they belong to the primary vertex or the B decay vertex: the track probability $\mathcal{P}_T$ as obtained from the signed impact parameter and the rapidity computed relative to the jet axis. The different rapidity distributions for particles from B decays compared to particles from the primary fragmentation process (see Fig. 19) can also be used to classify neutral particles.

[2]Throughout the paper N_B and N_{B^*} refer to the number of primary $B^{(*)}$ mesons

The different experiments have developed several techniques to reconstruct the B hadron momentum vector. ALEPH uses the track probability $\mathcal{P}_T$ as obtained from the signed impact parameter for the charged particles and rapidity for the neutral particles. DELPHI employs only rapidity for charged and neutral particles. OPAL uses inclusive reconstructed secondary vertices for the charged particles and the electromagnetic energy in 23° cone around the jet axis for the neutral particles. To account for neutrino losses, detector inefficiencies and wrong mass assignments a correction dependent on the measured B hadron mass and relative jet energy is applied, as determined from the Monte Carlo simulation. This improves the relative B momentum resolution significantly. The typical resolution for the reconstructed B momentum is $\sigma(P_b)/P_b \approx 7\% - 10\%$ plus a non Gaussian tail for $(10 - 20)\%$ of the B hadron candidates. The direction is reconstructed with a resolution of $\sigma(\Phi) \approx \sigma(\Theta) \approx (14 - 20)\ mrad$.

DELPHI [50] has used the inclusive B hadron momentum reconstruction to measure the fragmentation function of the various B meson states (see Fig. 20). The average B energy, scaled to the beam energy is found to be $< x_E >_b = 0.716 \pm 0.0006 \pm 0.007$ and the shapes of the fragmentation functions are in good agreement with expectation from the JETSET Monte Carlo simulation.

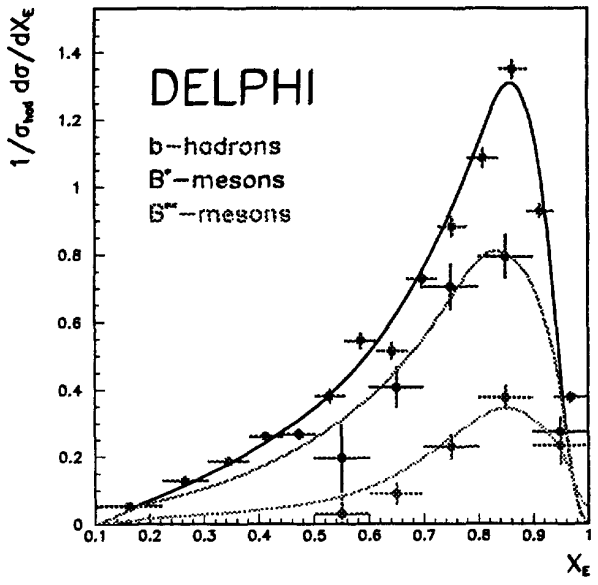

Figure 20: B hadron fragmentation function as measured by DELPHI.

2.2 B^* Production

L3 was the first LEP experiment that reported the observation of $B^* \to B\gamma$ decays [51]. As the only LEP experiment they could use their excellent electromagnetic calorimeter to reconstruct the low energetic photons from this decay. The B hadron boost was fixed to 37 GeV/c and the B flight direction was approximated by the JET direction, leading to a resolution of only 35 mrad. The relative B^* production rate in e^+e^- annihilation was measured for the first time to be:

$$\frac{N(B^*)}{N(B)+N(B^*)} = (76 \pm 8 \pm 6)\ \% \tag{2}$$

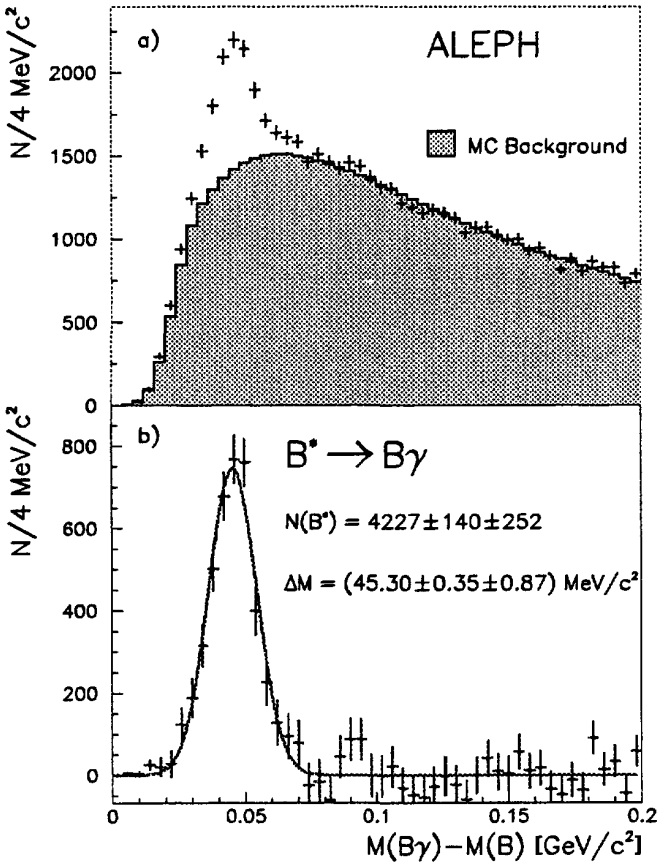

Figure 21: (a) The $B\gamma$-B-mass difference as measured by ALEPH. The background estimated from the Monte Carlo simulation, normalised to the same number of $q\bar{q}$-events, is shown by the hatched area. (b) The background subtracted signal for the decay $B^* \to B\gamma$ fitted with a Gaussian (curve).

Similar analysis have been performed by ALEPH [52] and DELPHI [53]. Different to L3, converted photons have been used to reconstruct the low energetic

photon from the $B^* \to B\gamma$ decay. Using better algorithms to reconstruct the B hadron momentum vector (see Chap. 2.1) they where also able to measure the $B^* - B$ mass difference, as seen in Fig. 21.

2.3 B^* Polarisation

The decay angle distribution of the photon in the B^* rest frame θ^* has been measured by ALEPH [52] and DELPHI [53]. It can be used to distinguish between transverse (helicity ± 1) and longitudinal (helicity 0) polarised B^* mesons, which have the differential cross sections $\sigma_T \propto (1 + \cos^2\theta^*)/2$ and $\sigma_L \propto \sin^2\theta^*$ respectively. If the helicity states are equally populated, i.e. $\sigma_T : \sigma_L = 2 : 1$, a flat helicity angle distribution is expected.

The relative longitudinal contribution is determined from the fit of the decay angle distribution (see Fig. 22) to be $\sigma_L/(\sigma_L + \sigma_T) = (33 \pm 6 \pm 5)\%$, in agreement with the expectation of 1/3 for equally populated helicity states.

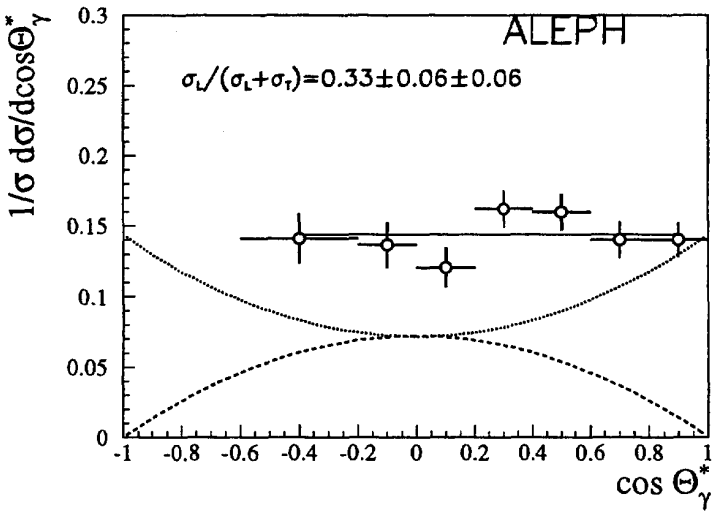

Figure 22: The acceptance-corrected number of B^*-mesons as a function of the photon decay angle ($\cos\theta^*$) in the B^* rest frame. The dashed and the dotted curves are the contributions from the transverse and longitudinal polarised states. The fit of both contributions to the data points is given by the solid curve.

2.4 B^{**} Production

For the B^{**} search, the photon is replaced by a charged pion. This pion is called in the following π^{**}. The photon from the decay $B^{**} \to B^*\pi^{\pm}, B^* \to B\gamma$ is lost. Only a small fraction of B^* mesons ($\approx 10\%$) are expected to originate from B^{**} decays. Therefore the search for B^{**} states starting with a reconstructed $B^* \to B\gamma, \gamma \to e^+e^-$ decay would reduce the signal by a large factor but not affect the background level. Also no improvement for the signal width is expected, due to the fact that the photon is of such low energy compared to the π^{**} in the B^{**} rest frame that the photon lost in the decay chain only shifts the effective mass of the $(B\pi^{\pm})$ system down by 46 MeV/c^2 from the true B^{**} mass, but does not broaden the signal significantly.

The B^{**} has a negligible lifetime compared to the average B hadron. This allows one to reduce the combinatorial background using the signed impact parameter to distinguish between tracks from the primary vertex and tracks originating from the long lived B hadron decay (see Fig. 23).

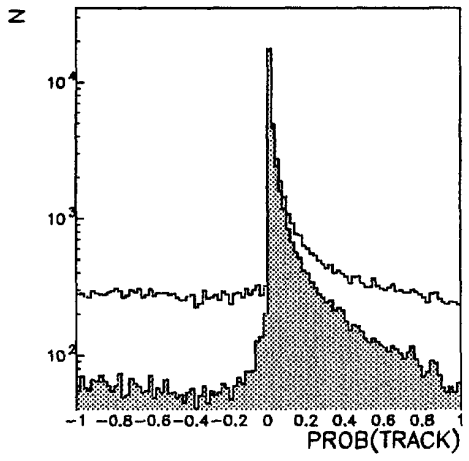

Figure 23: Probability distribution for charged track to stem from the primary vertex computed from the signed impact parameter significance. The probability is signed according to the sign of the impact parameter. The shaded area shows the contribution of the tracks from B hadron decays.

The ALEPH [52] signal for B^{**} states is shown in Fig. 24. Within the experimental resolution for the inclusive B hadron momentum reconstruction it is not possible to resolve the expected four different $B^{**}_{u,d}$ states. ALEPH has also observed B^{**} states combining fully reconstructed B hadron decays with charged pions from the primary vertex [54]. Unfortunately this analysis is limited by

the available statistics and is therefore also not able to resolve the masses and productions rates for the four expected $B^{**}_{u,d}$ states.

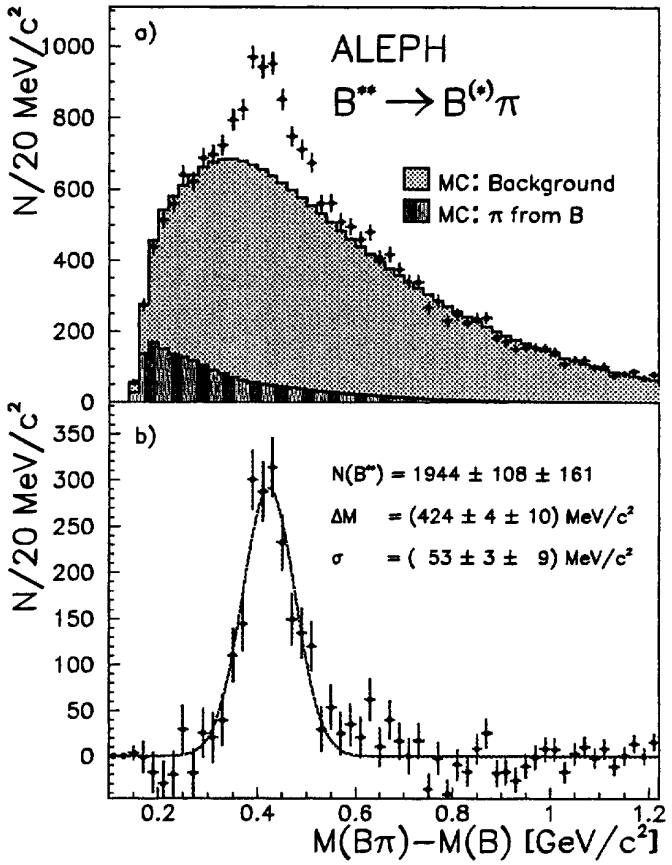

Figure 24: a) The $(B\pi)$ – B-mass difference as measured by ALEPH. The background estimated from the Monte Carlo simulation is shown by the hatched area. (b) The background-subtracted signal for the decay $B^{**} \to B^{(*)}\pi^{\pm}$ fitted with a Gaussian (curve).

The first LEP experiments which reported evidence for B^{**} states was OPAL [55]. Using inclusive reconstructed secondary vertices they are able to distinguish with good purity between B^+ and B^0 candidates (see Fig. 25). Using the charge correlation in $B^{0**} \to B^+\pi^-$ decays they could prove the existence of B^{**} states since they where able to cross check the JETSET Monte Carlo simulation for the background with the wrong charge combination (see Fig. 27).

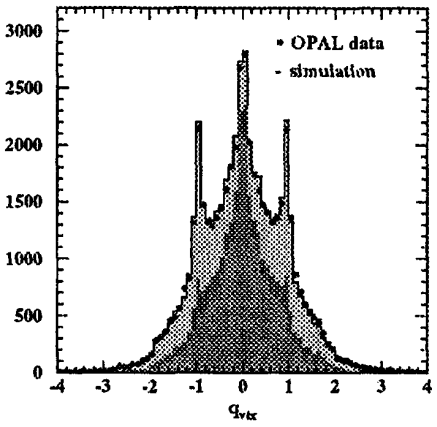

Figure 25: Secondary vertex charge as measured by OPAL in select B events.

With the same method, but now with charged tracks identified as kaons by dE/dx, B_s^{**} states have been observed (see Fig. 27) with a relative production rate of

$$\frac{BR(Z \to \bar{b} \to B_s^{**0} \to B^{(*)+}K^-)}{BR(Z^0 \to \bar{b} \to B^+)} = 0.026 \pm 0.008$$

and a mass of $M(B_s^{**}) = (5884 \pm 15)\ MeV/c^2$. Evidence for these states has also been reported by DELPHI [57]. One should note that a large B_s^{**} production rate reduces significantly the number of B_s mesons for which $B_s^0 \bar{B}_s^0$ oscillations can be observed (see Fig. 26).

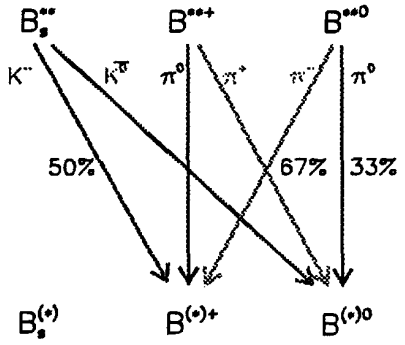

Figure 26: Expected B^{**} decay modes.

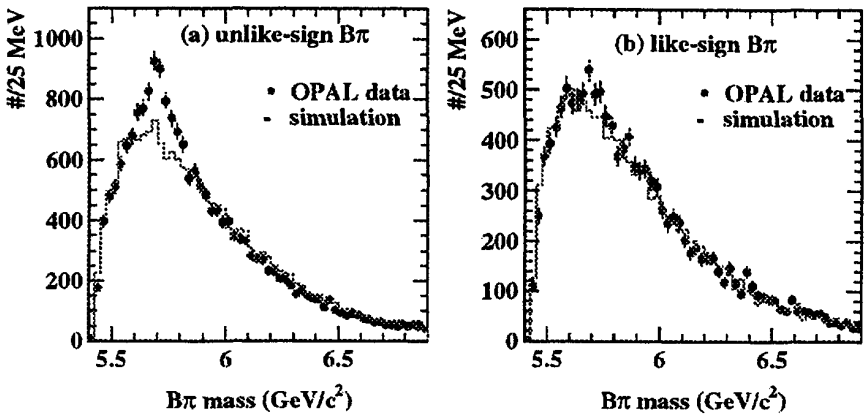

Figure 27: B^{**} signal from OPAL: (a) right charge $B\pi$ combinations. (b) wrong charge $B\pi$ combinations.

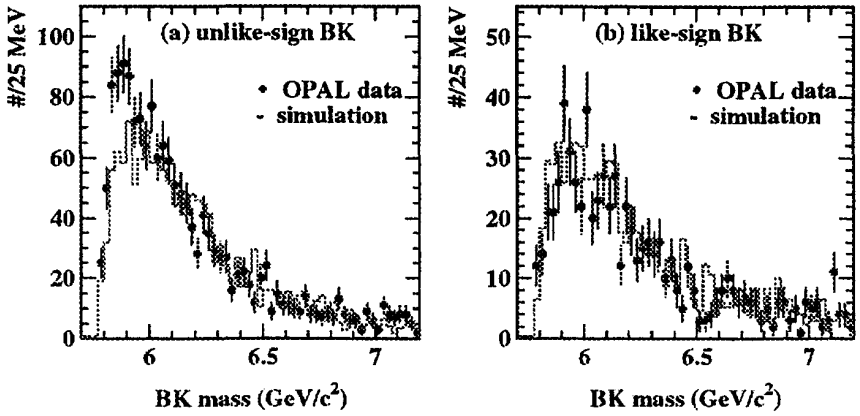

Figure 28: B_s^{**} signal from OPAL. (a) right charge BK combinations. (b) wrong charge BK combinations.

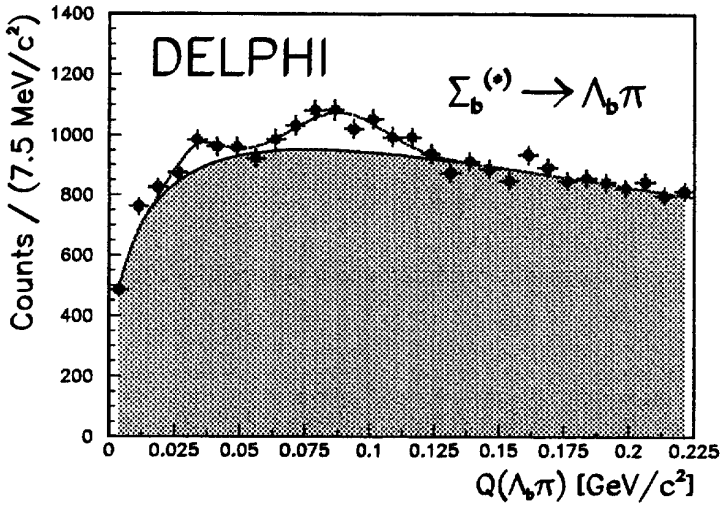

Figure 29: $\Sigma_b^{(*)}$ signal from DELPHI ($Q(\Lambda_b\pi) = m(\Lambda_b\pi) - m(\Lambda_b) - m(\pi)$). The expected background from the Monte Carlo simulation is shown by the shaded area.

In order to find $\Sigma_b^{(*)} \rightarrow \Lambda_b\pi^{\pm}$ decays DELPHI [58] uses an B baryon enriched event sample. Therefore events are selected with an identified fast proton or Λ from the primary fragmentation process. The observed signal is shown in Fig. 29. The following mass differences relative to the Λ_b are measured:

$$\begin{aligned} m(\Sigma_b^{\pm}) - m(\Lambda_b) &= (173 \pm 3 \pm 8)\ MeV/c^2 \\ m(\Sigma_b^{*\pm}) - m(\Lambda_b) &= (229 \pm 3 \pm 8)\ MeV/c^2 \end{aligned}$$

in agreement with recent calculations. The relative production rate is measured to be:

$$\frac{\sigma(\Sigma_b) + \sigma(\Sigma_b^*)}{\sigma_b} = 0.048 \pm 0.006 \pm 0.015$$

One should note, that a large Σ_b production rate could reduce significantly the expected Λ_b polarisation.

2.5 Excited Beauty States Summary

The measurements of the B^* mass and production rate are summarised in Fig. 30. The LEP measurements have reached a similar precision for the mass difference as compared to the previous world average [2]. The relative production rate of $N(B^*)/(N(B) + N(B^*)) = (75 \pm 4)\%$ is in good agreement with the expectation

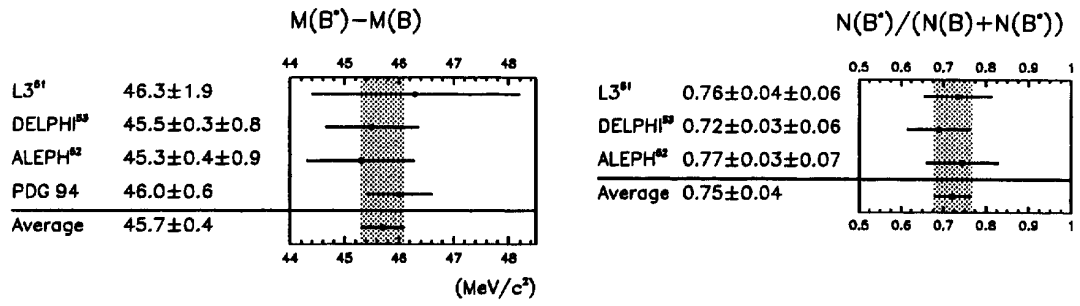

Figure 30: Measurements of the B^* mass and relative production rate.

from spin counting.

B^{**} states have been experimentally established by OPAL [55], DELPHI [56] and ALEPH [52] [54]. A large production rate for B^{**} states has been observed by all experiments (see Fig. 31). An initial B flavour tag for a CP violation measurement based on the charge of the pion from a $B^{**+} \to B^0\pi^+$ decay could therefore be interesting for future CP violation measurements at CDF or LHC. The average mass of the B^{**} states is in good agreement between the experiments (see Fig. 31). None of the experiments is able to resolve the four expected B^{**} states. In principal CDF should be able to do this with their large sample of fully reconstructed B decays.

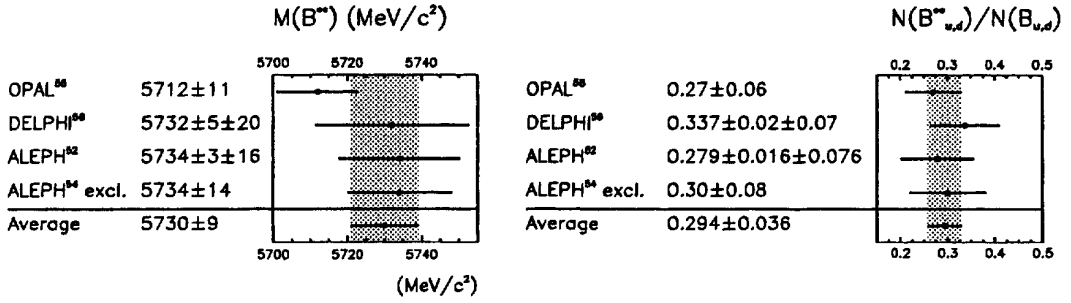

Figure 31: Measurements of the $B^{**}_{u,d}$ mass and relative production rate.

3 $B\bar{B}$-Oscillations

The decay of the weak eigenstates B^0 and $\bar{B}^0$ is described by the Schrödinger equation:

$$i\frac{\partial}{\partial t}\begin{pmatrix}|B^0>\\|\bar{B}^0>\end{pmatrix} = \left[\begin{pmatrix}M & M_{12}\\ M_{12}^* & M\end{pmatrix} - \frac{i}{2}\begin{pmatrix}\Gamma & \Gamma_{12}\\ \Gamma_{12}^* & \Gamma\end{pmatrix}\right]\begin{pmatrix}|B^0>\\|\bar{B}^0>\end{pmatrix} \qquad (3)$$

with M being the mass of the weak eigenstates B^0 and $\bar{B}^0$ and Γ their decay width. Responsible for $B^0 - \bar{B}^0$ oscillations are the off diagonal elements M_{12} and Γ_{12}. The two CP eigenstates $B_{1,2} = \frac{1}{\sqrt{2}}(B^0 \pm \bar{B}^0)$ with masses $M_{1,2} = M \pm \Delta m/2$ and width $\Gamma_{1,2} = \Gamma \pm \Delta\Gamma/2$ are obtained from the diagonalisation of the decay matrix. They are equivalent to the mass eigenstates if CP is conserved. The consequence of Eq. 3 is that an initially pure B^0 state can decay either as a B^0 or a $\bar{B}^0$. The probabilities can be computed from Eq. 3

$$\begin{aligned}\mathcal{P}(B^0) &= e^{-t/\tau}\cdot\frac{(1+\cos\Delta mt)}{2}\\ \mathcal{P}(\bar{B}^0) &= e^{-t/\tau}\cdot\frac{(1-\cos\Delta mt)}{2}\end{aligned}$$

and are shown for two different values of ΔM in Fig. 32.

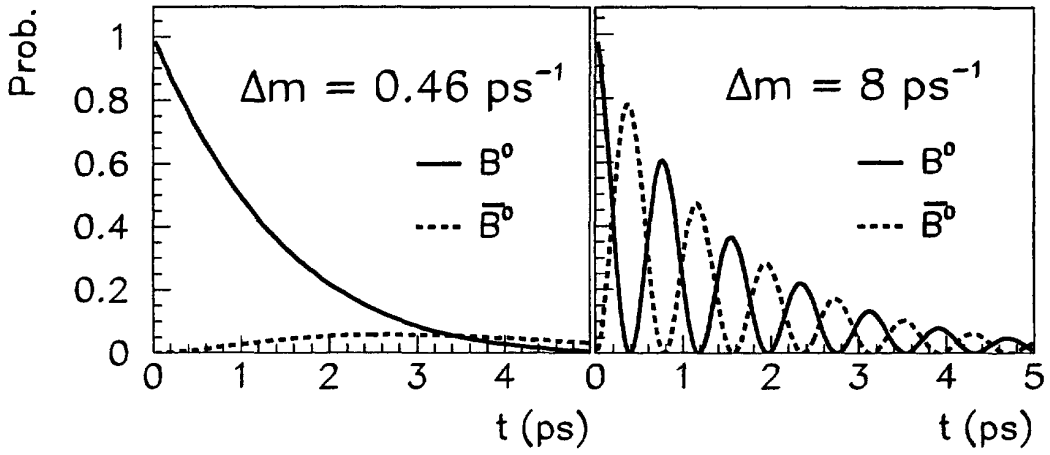

Figure 32: $B\bar{B}$ oscillations for two different values of ΔM.

In the framework of the Standard Model M_{12} and Γ_{12} can be calculated [59]. The particle-antiparticle oscillations proceed by a second order weak interaction, dominated by a top quark exchange, as shown in Fig. 33. In this framework the lifetime difference for the two B_d^0 states is predicted to be small: $\left(\frac{\Delta\Gamma}{\Gamma}\right)_{B_d} \leq 1$ %

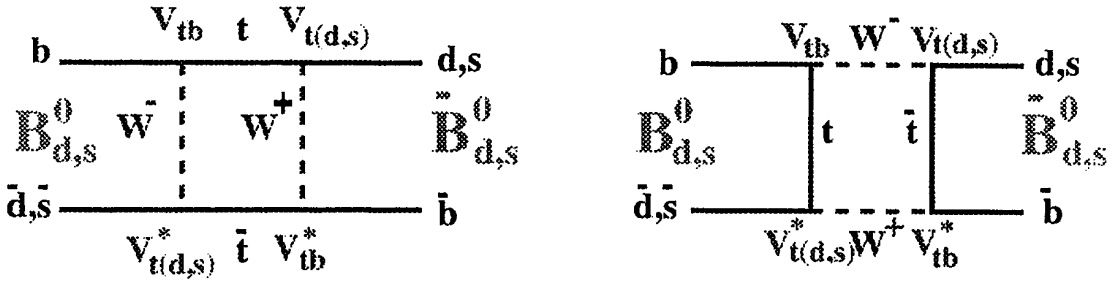

Figure 33: Box diagrams for $B^0\bar{B}^0$ transitions.

while for the B_s^0 one expects: $\left(\frac{\Delta\Gamma}{\Gamma}\right)_{B_s}$ $10-20$ %. One should note, that it could well be that this is the largest lifetime difference in the B meson sector.

The mass difference Δm is given by:

$$\Delta m_q = \frac{G_F^2}{6\pi^2} \cdot m_{B_q} \cdot m_t^2 \cdot F(\frac{m_t^2}{m_W^2}) \cdot \eta_{QCD} \cdot B_{B_q} \cdot f_B^2 \cdot |V_{tb}^* V_{tq}|^2 \qquad (4)$$

where G_F is the Fermi constant, m_{B_q} is the B meson mass (m_{B_d} or m_{B_s}), m_t is the top quark mass, m_W is the W boson mass, η_{QCD} represents short distance QCD corrections, B_{B_q} is the B bag parameter, f_B is the B decay constant and V_{tb} and V_{td} (V_{ts}) are the CKM matrix elements involved in $B_d^0\bar{B}_d^0$ ($B_s^0\bar{B}_s^0$) oscillations.

Unfortunately some of the quantities in Eq. 4 such as η_{QCD}, B_{B_q} and f_B are poorly known for the time being. Therefore our knowledge about V_{td} from the precise B_d^0 oscillation measurements is still limited. However, most of these uncertainties cancel in the ratio [60]

$$\frac{\Delta m_s}{\Delta m_d} = \frac{m_{B_s}}{m_{B_d}}(1.15 \pm 0.05)\left|\frac{V_{ts}}{V_{td}}\right|^2 \qquad (5)$$

which makes it very important to measure also $B_s^0\bar{B}_s^0$ oscillations. Together with the existing measurements of the B semileptonic branching-ratios ($b \to cl\nu$ and $b \to ul\nu$), this would allow to determine the unitarity triangle (see Fig. 34) of the CKM-matrix completely, if $|V_{cb}| = |V_{ts}|$ is assumed. The knowledge of the three angles of the unitarity triangle would then give precise predictions for the CP violation expected in the B sector in the framework of the standard model.

3.1 Time integrated measurements

The first observation of $B_d^0\bar{B}_d^0$ oscillation was made by ARGUS [61] at the $\Upsilon(4S)$ resonance. They used the time integrated observable χ defined as:

$$\chi = \int_0^\infty \mathcal{P}_{B^0\to\bar{B}^0}(t)dt = \frac{1}{2}\,\frac{(\Delta m/\Gamma)^2}{1+(\Delta m/\Gamma)^2} = \frac{1}{2}\,\frac{x^2}{1+x^2}$$

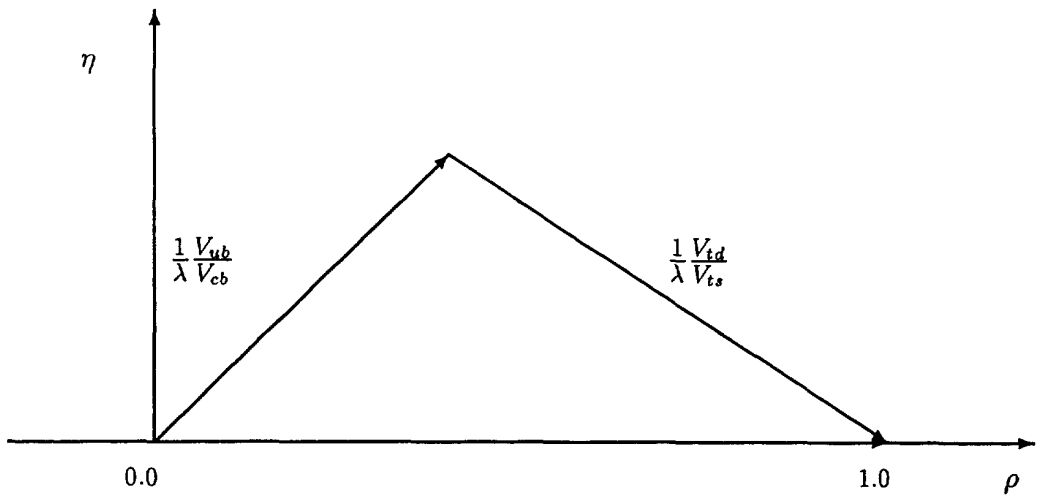

Figure 34: Unitarity triangle of the CKM Matrix in the ρ, η-plane with $\lambda \approx |V_{us}|$.

where $x = \Delta m/\Gamma$. Both at the $\Upsilon(4S)$ and at the Z B hadrons are produced in pairs. A B meson decays into $B^0(\bar{b}, d) \to D^{(*)-}(\bar{c}, d)l^+\nu$ while a $\bar{B}$ meson decays into $\bar{B}^0(b, \bar{d}) \to D^{(*)+}(c, \bar{d})l^-\nu$. The experimental signatures which have been used by all $B^0\bar{B}^0$ oscillation measurements up to now are therefore like-sign lepton pairs or unlike-sign lepton $D^{(*)}$ combinations. The fraction of mixed events (R) is defined as:

$$\begin{aligned} R &= \frac{N^{mix}}{N^{mix} + N^{unmix}} \\ &= \frac{N(l^{\pm}l^{\pm})}{N(ll)} \qquad \text{lepton} - \text{lepton tag} \\ &= \frac{N(D^{(*)\pm}l^{\mp})}{N(D^{(*)}l)} \qquad D^{(*)} - \text{lepton tag} \end{aligned} \tag{6}$$

In the decay of the $\Upsilon(4S) \to B^0\bar{B}^0$ the B meson pair is produced coherently in a $l = 1$ ($C = -1$) state. For this case χ is given by:

$$\chi = \left[1 + \frac{f_+}{f_0}\left(\frac{\tau_+}{\tau_0}\right)^2\right] \cdot R \tag{7}$$

where f_+ and f_0 are the B^+ and B^0 production rates and τ_+ and τ_0 their lifetimes. N^{mix} and N^{unmix} are measured using lepton-lepton correlations and $D^{(*)}$-lepton correlations by ARGUS and CLEO. Nothing new was presented this summer. The world average is [62]: $\chi_d = 0.167 \pm 0.025$. The measurements are dominated by the systematic uncertainties in $f_{+,0}$ and $\tau_{+,0}$.

At LEP, the two B mesons are produced in an incoherent state and therefore $R \propto 2\chi(1-\chi)$. Different to the $\Upsilon(4S)$ not only B^+ and B_d^0 mesons are produced

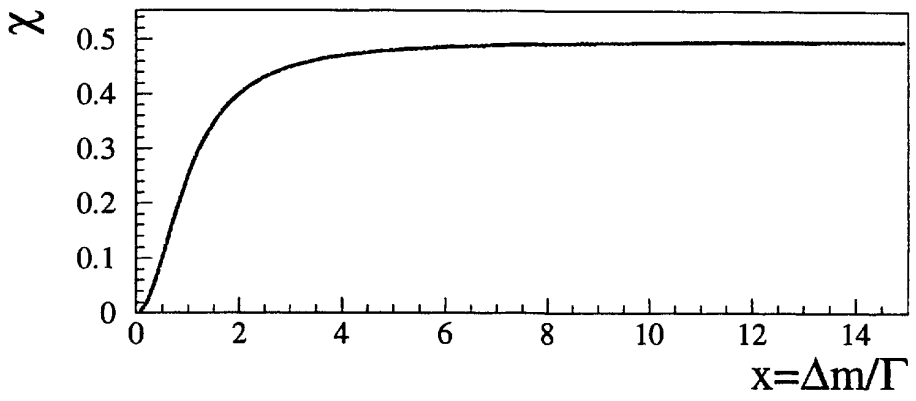

Figure 35: χ as a function of $x = \Delta m/\Gamma$.

in $Z \to b\bar{b}$ decays but also B_s^0 mesons. The quantity which is therefore measured at LEP is [62]:

$$\bar{\chi} = f_d\chi_d + f_s\chi_s = 0.115 \pm 0.006 \tag{8}$$

where f_d and f_s are the B_d^0 and B_s^0 meson production rates. Similar experimental signatures are used in these analysis as at the $\Upsilon(4S)$.

Using the measurements of the B semileptonic branching ratios $b \to cl\nu$ and $b \to ul\nu$, the value of χ_d and the strength of the CP violation in the K^0 system (ϵ), the unitarity triangle (see Fig. 34) can be used to predict Δm_s [60].The preferred range is 8.6 $ps^{-1} \leq \Delta m_s \leq 17\ ps^{-1}$. It can easily been seen (Fig. 35) that χ is insensitive to large values of $x = \Delta m/\Gamma$. New techniques have therefore been developed at LEP to resolve the time structure in $B^0\bar{B}^0$ oscillations.

3.2 $B_d^0\bar{B}_d^0$ oscillations

A schematic view of a $Z \to b\bar{b}$ event is shown in Fig. 36. The flavour of the B meson at decay time is identified by the $D^{*+} \to D^0\pi^+$ decay. The flavour at the production time can either be measured using a lepton from a semileptonic decay in the opposite hemisphere or by jet charge techniques. The jet charge is defined by:

$$Q_{jet} = \frac{\sum_i |\vec{p_i} \cdot \vec{e_J}|^\kappa \cdot q_i}{\sum_i |\vec{p_i} \cdot \vec{e_J}|^\kappa} \tag{9}$$

where $\vec{p_i}$ are the momentum vectors of the particles with charge q_i in the jet and $\vec{e_J}$ is the unity vector along the jet direction. The weights κ are choosen to give an optimal charge reconstruction and are different in the various analysis.

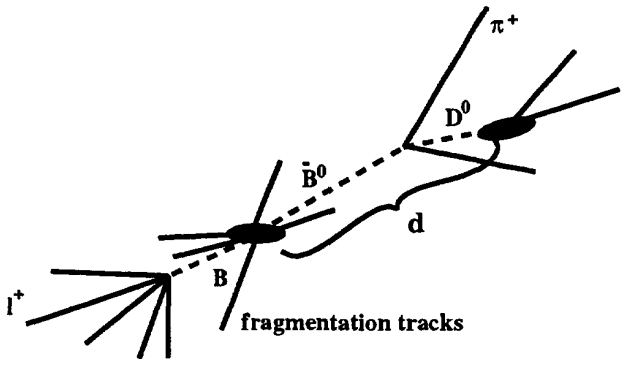

Figure 36: Schematic view of a $Z \to b\bar{b}$ event.

To measure the oscillation rate as a function of the proper time one needs a measurement of both the decay length d_B and momentum p_B, since $t = d/\gamma\beta = d \cdot m_B/p_B$. The proper-time resolution is then the sum of the two terms:

$$\frac{\sigma_t}{\tau} = \frac{\sigma_d}{< d >} \oplus \frac{\sigma_p}{p}\frac{t}{\tau} \tag{10}$$

where $< d >$ is the average B flight length, which is 2.5 mm at LEP. The B_d^0 meson decay length (d) is taken from the reconstructed charm vertex and the B momentum is estimated from the (D^*l) momentum using Monte Carlo models. The typical momentum resolution is $\sigma_p/p = (10 - 20)\%$ and the decay length resolution is $\sigma_d \approx 300\mu m = 0.2ps$. Such analysis have been performed by ALEPH [63], DELPHI [64] and OPAL [65]. The result from OPAL is shown in Fig. 38. The time dependent fraction of like sign events R is given by:

$$R(t) = \frac{N_{mix}(t) - N_{mix}^{bck}(t)}{N_{tot}(t) - N_{tot}^{bck}(t)} \tag{11}$$

$$= \omega + (1 - 2\omega)\frac{1 - \cos\Delta m_d t}{2} \tag{12}$$

where ω is the fraction of incorrectly tagged events. A clear oscillation pattern is observed and a value of $\Delta m_d = (0.539 \pm 0.060 \pm 0.024)\ ps^{-1}$ is measured.

Also events with two semileptonic B decays (see Fig. 37) have been used to measure the time dependent $B^0\bar{B}^0$ oscillation rate. The B decay vertex is reconstructed here with an inclusive secondary vertex search starting with the identified lepton. ALEPH [63], DELPHI [64] and OPAL [66] have used inclusive techniques to reconstruct the B boost while L3 uses $P_B = 0.85 \cdot E_{beam}$. This works rather well due to the hard B fragmentation function. L3 [68] finds 1107 di-lepton

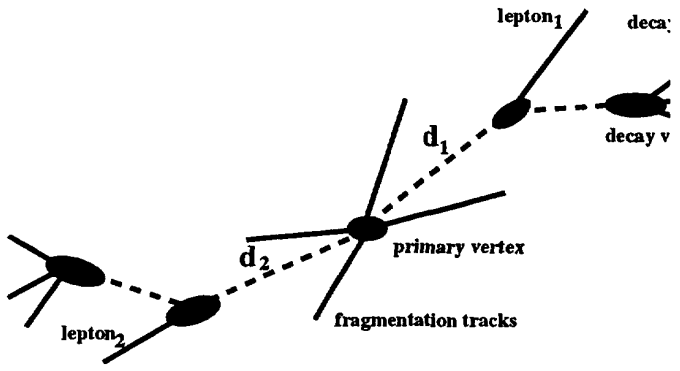

Figure 37: Schematic view of a $Z \to b\bar{b}$ event with two semileptonic B decays.

events in a sample of 1.5 million hadronic Z decays. They are able to reconstruct 1429 secondary vertices in this sample. From the fraction of the like-sign lepton pairs (see Fig. 39) they measure: $\Delta m_d = (0.496^{+0.055}_{-0.051} \pm 0.043)\ ps^{-1}$.

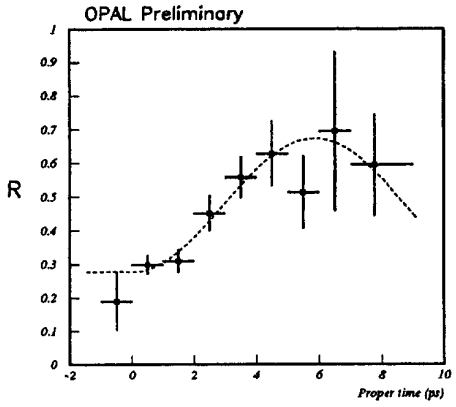

Figure 38: Like-sign fraction versus proper time, for the D^*-tagged analysis from OPAL.

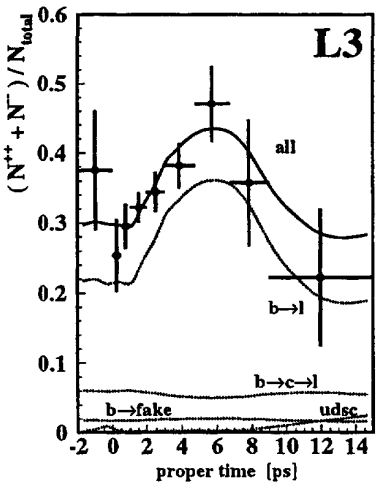

Figure 39: Like-sign fraction versus proper time, for the ll-tagged analysis from L3.

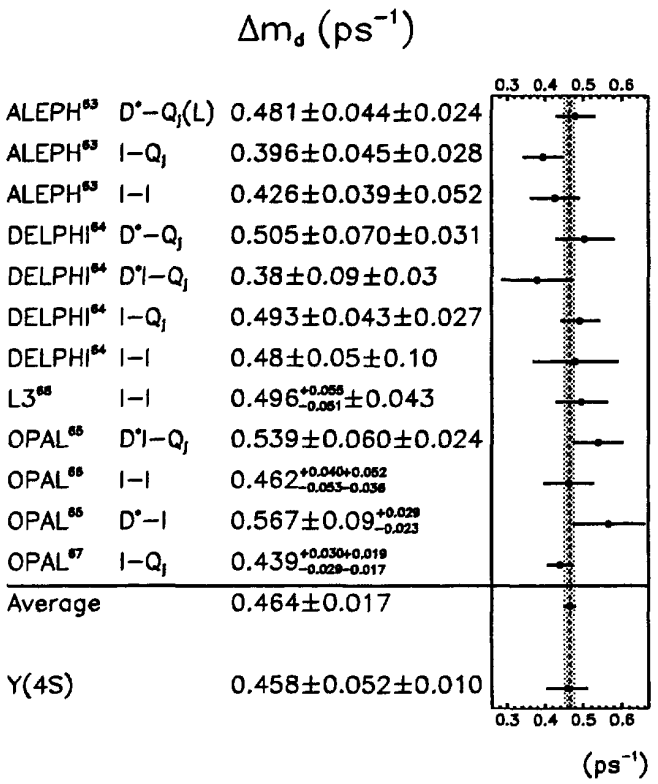

Figure 40: Summary of the Δm_d measurements. A B_d^0 lifetime of $\tau(B_d^0) = (1.545 \pm 0.033)\ ps$ has been used to compute Δm_d from the measured value of χ_d at the $\Upsilon(4S)$. The uncertainty in the B_d^0 lifetime is the origin of the third error quoted.

The measurements of Δm_d from the LEP experiments are summarised in Fig. 40. The LEP average of $\Delta m_d = (0.464 \pm 0.017)\ ps^{-1} = (3.05 \pm 0.11) \cdot 10^{-4}\ eV/c^2$ has reached a precision of 4% which is much better than the time integrated measurements at the $\Upsilon(4S)$.

3.3 $B_s^0\bar{B}_s^0$ oscillations

The measurement from LEP of $\bar{\chi} = f_d\chi_d + f_s\chi_s = 0.115 \pm 0.006$ can be used to constrain χ_s experimentally. The LEP average for Δm_d gives a value of $\chi_d = 0.170 \pm 0.009$ using a B_d^0 lifetime of $\tau(B_d^0) = (1.545 \pm 0.033)$ ps. The B_d^0 and B_s^0 production rates in Z decays have also been measured: $f_d = (38.8 \pm 1.3 \pm 2.1)\%$ and $f_s = (11.0 \pm 1.2^{+2.5}_{-2.6})\%$ [69]. The experimental situation is summarised in Fig. 41 leading to the lower limit of $\chi_s \geq 0.29$ with 95% CL. If one uses on the other hand the constraint from the unitarity triangle of the CKM matrix that $12.9 < x_s < 26.1$ [60], which corresponds to $\chi_s = 0.5$, one can determine the B_s meson production rate in Z decays, $f_s = (10.2 \pm 1.6)\%$, with a better accuracy than from the measurement quoted above. The knowledge of f_s is one of the key inputs for any measurement of $B_s^0\bar{B}_s^0$ oscillations in Z decays.

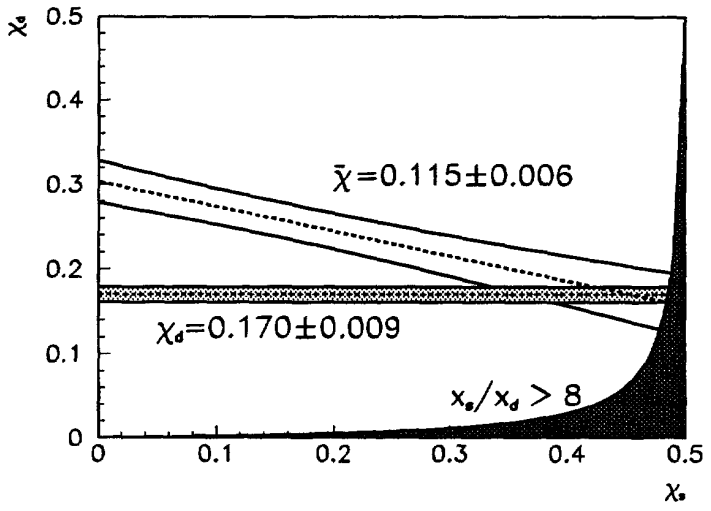

Figure 41: Constraints on the (χ_d,χ_s) plane. The shaded area shows the constraint from the CKM unitarity triangle.

Evidence for $B_s^0\bar{B}_s^0$ oscillations has been observed by ALEPH [70] in one of its handful fully reconstructed B_s^0 decays. (Fig. 42). The identified K^+ in the same hemisphere and the e^- in the opposite hemisphere tag the production state of a B_s^0 meson which decays then as $\bar{B}_s^0 \to D_s^+\pi^-$. Unfortunately the statistics of fully reconstructed B_s^0 decays at LEP is too small to measure the oscillation frequency.

The di-lepton analysis presented in the previous section is also sensitive to $B_s^0\bar{B}_s^0$ oscillations. The like-sign fraction as a function of proper time from

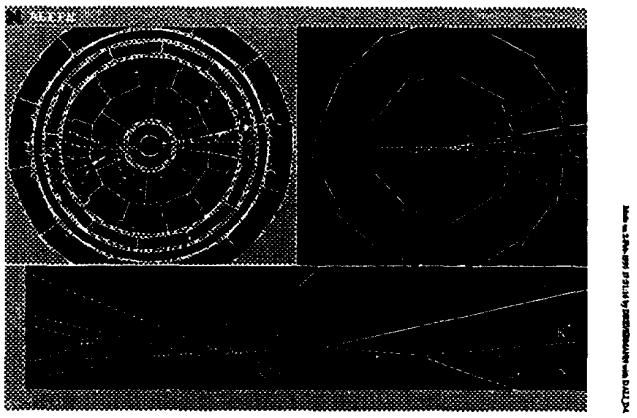

Figure 42: A fully reconstructed $\bar{B}_s^0 \to D_s^+\pi^-$ decay from ALEPH, where the B_s^0 oscillates to a $\bar{B}_s^0$ before decaying.

ALEPH [63] is shown in Fig. 43. In the blown up region in the lower left corner a fit to the data points is shown with a second oscillation frequency $\Delta m_s = 8.4\ ps^{-1}$. From a data sample of nearly 10000 leptons with a proper time measurement no signal for $B_s^0\bar{B}_s^0$ oscillations is observed. Monte Carlo techniques are used to set a lower limit of $\Delta m_s \geq 5.6\ ps^{-1}$ at 95% CL (see Fig. 43).

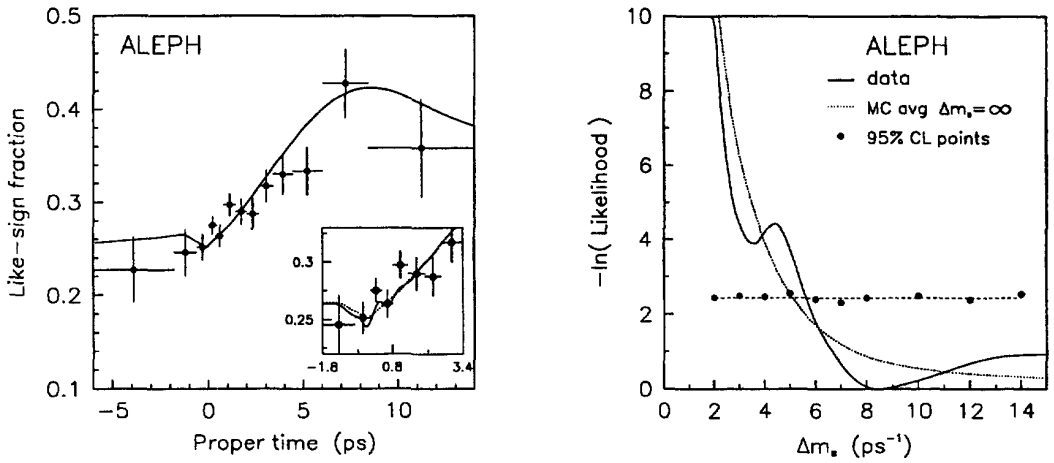

Figure 43: Left: Like-sign fraction versus proper time from di-lepton events measured by ALEPH. The curve shows a fit to the data points with Δm_d as free parameter and maximal $B_s^0\bar{B}_s^0$ mixing. The blown up region shows a fit where $\Delta m_s = 8.4\ ps^{-1}$ is used. Right: Log likelihood function for the di-lepton analysis from ALEPH.

Similar to the technique used for the measurement of Δm_d with $(D^{(*)}l)$-events $(D_s l)$-events can be used to measure Δm_s. Such an event is shown from the ALEPH event display in Fig. 44. The B_s^0 flavour at the decay time is given

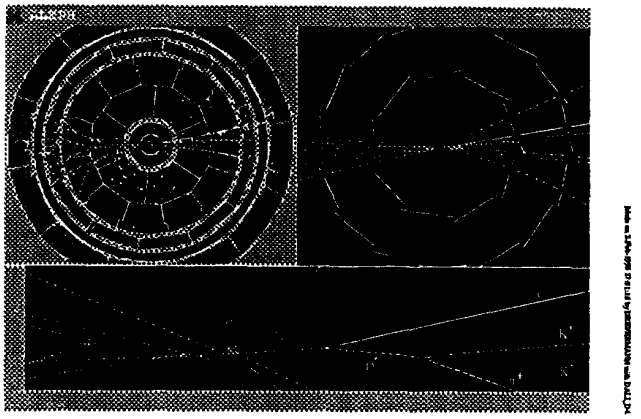

Figure 44: A $\bar{B}_s^0 \to D_s^+ l\nu$ decay from ALEPH.

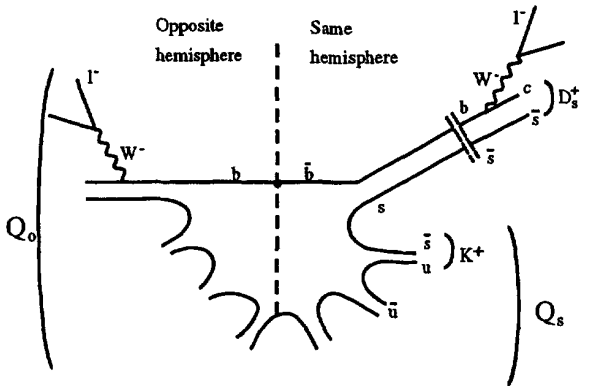

Figure 45: Schematic view of a $Z \to b\bar{b}$ event. The different possibilities to identify the B_s^0 flavour at the production time are indicated.

by the D_s and the lepton charge. To determine the B_s^0 flavour at the production time several observables are used (see Fig. 45). The preferred tag is a fast lepton in the opposite hemisphere. If this is not found, a fast kaon in the same hemisphere determines also the B_s^0 flavour at the production time. In a sizeable fraction of the events with $D_s l$ combination none of the above can be found. In this case the jet charge in the same- and in the opposite hemisphere is used.

ALEPH [71] reconstructs 277 $D_s l$ combinations from 4 million Z decays using 7 different D_s decay modes. The likelihood function (see Fig. 46) indicates that low values of Δm_s are strongly disfavoured but that no signal value of Δm_s is significantly preferred. A lower limit of $\Delta m_s > 6.6\ ps^{-1}$ at 95 % CL is obtained.

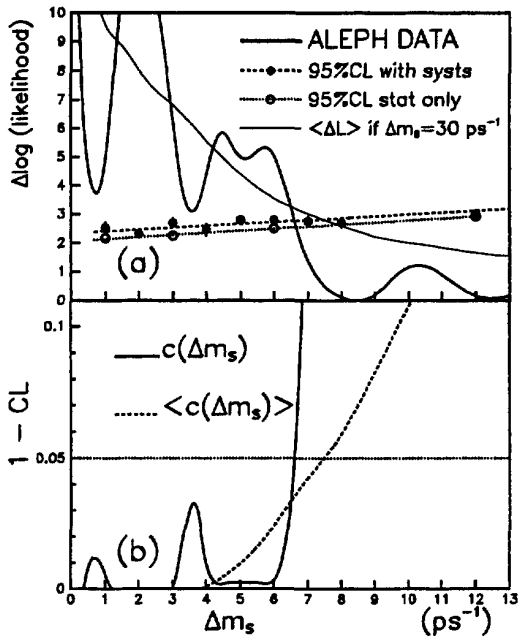

Figure 46: a) $\Delta L(\Delta m_s)$ from the ALEPH $D_s l$ analysis. b) The solid curve shows 1-CL determined from the data and fast Monte Carlo simulations to include systematic uncertainties. The dashed curve shows the average behaviour expected for $\Delta m_s = 30\ ps^{-1}$.

The limits for the $B_s^0 \bar{B}_s^0$ oscillation frequency Δm_s are summarised in Fig. 47. None of the LEP experiments observed $B_s^0 \bar{B}_s^0$ oscillations. A mathematical procedure has been proposed [75] to be able to combine the limits from the various experiments. Even within one experiment this is a non trivial task since the different analysis are statistically and systematically correlated. ALEPH [76] presented this summer a combined limit of $\Delta m_s > 7.8\ ps^{-1}$ at 95% CL. The work to combine the Δm_s measurements from all LEP experiments is still going on, a preliminary result [77] of $\Delta m_s > 9.5$ at 95% CL has already been shown. Using the world average of $\tau(B_s) = 1.52 \pm 0.07\ ps$ this corresponds to $x_s > 14.4$.

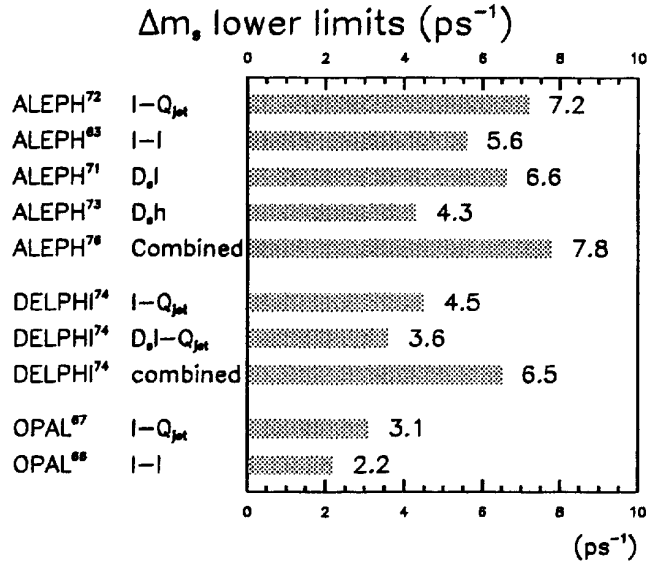

Figure 47: The limits on Δm_s from the LEP experiments.

3.4 $B - \bar{B}$ oscillations summary

The capability to resolve the time structure of $B_d^0 - \bar{B}_d^0$ oscillations at LEP improved the precision of the Δm_d measurements during the last years significantly. The measurement $\Delta m_d = (0.464 \pm 0.017)\ ps^{-1}$ has reached an impressive precision of 3.6%. In combination with the lower limit of $\Delta m_s > 9.5\ ps^{-1}$ @95% CL one gets from Eq. 5:

$$\left|\frac{V_{ts}}{V_{td}}\right| > 3.8\ @\ 95\%\ CL \tag{13}$$

This constraints the upper length of the right side of the unitarity triangle and starts to cut into the region which is still allowed by the other measurements. It is not very likely that one of the LEP experiments will be able to observe $B_s^0 \bar{B}_s^0$ oscillations since the data taking period for LEP I is over and the preferred value [60] of $\Delta m_s = (12.1 \pm 2.1) \frac{f_{B_s}^2 B_{B_s}}{(230 MeV)^2}\ ps^{-1}$ is beyond the reach of the current analysis techniques. Unless new and more powerful methods to analyse $Z \to b\bar{b}$ events are invented, the community will have to wait for BaBar, HERA-B and the LHC experiments to measure Δm_s. In combination with the measurement of the CP violation in the B_d^0 decay to $J/\Psi K_S^0$, this will then allow a real test of the unitarity of the CKM matrix and hence answer the question whether the world is built of more than 3 generations of quarks or not.

Acknowledgments

I am grateful to my colleagues on ALEPH and to the represantatives of the other experiments whoses results I have reviewed here, in particular R. Forty, H.G. Moser, M. Feindt and O. Podobrin. Congratualations to the CDF Collaboration for the excellant WWW page which provides all relevant information to review their impressive physics results. It is a pleasure to thank R. Settles for useful discussions.

References

References

[1] N. Isgur and M.B. Wise in *B Decays*, ed. S. Stone, (World Scientific, Singapore, 1994).

[2] R.M. Barnett *et al.*, *Phys. Rev.* D **54**, 1 (1996).

[3] M. Bauer, B. Stech, M. Wirbel, *Z. Phys.* C **34**, 103 (1987).

[4] I, Bigi *et al.* in *B Decays*, ed. S. Stone, (World Scientific, Singapore, 1994).

[5] D. Busculic *et al.*, ALEPH Collab., *Nucl. Instrum. Methods* A **360**, 481 (1995).

[6] J. Alcaraz *et al.*, "Averages of B Hadron Lifetimes", B Lifetime Group.

[7] R. Forty, CERN–PPE/94–144, 1994.

[8] D. Busculic *et al.*, ALEPH Collab., *Phys. Lett.* B **369**, 151 (1996).

[9] D. Busculic *et al.*, ALEPH Collab., *Phys. Lett.* B **314**, 459 (1993).

[10] P. Abreu *et al.*, DELPHI Collab., *Z. Phys.* C **63**, 3 (1994).

[11] P. Abreu *et al.*, DELPHI Collab., CERN–PPE/96–13, Submitted to Phys. Lett. **B**

[12] O. Adriani *et al.*, L3 Collab., *Phys. Lett.* B **317**, 474 (1993).

[13] O. Adriani *et al.*, L3 Collab., L3 Internal Note 1972.

[14] P.D.Acton *et al.*, OPAL Collab., *Z. Phys.* C **60**, 217 (1993).

[15] K. Abe *et al.*, SLD Collab., *Phys. Rev. Lett.* **75**, 3624 (1995).

[16] D. Buskulic et al., ALEPH Collab., CERN-PPE/96-14, Submitted to Z. Phys. **C**

[17] CDF Collab., http://www-cdf.fnal.gov/physics/new/bottom/bottom.html

[18] F. Abe et al., CDF Collab., Phys. Rev. Lett. **76**, (1996) 4462.

[19] P. Abreu et al., DELPHI Collab., Z. Phys. **C68** (1995) 13

[20] W. Adam et al., DELPHI Collab., Z. Phys. **C68** (1995) 363

[21] DELPHI Collab. "Accurate measurement of the B_d^0 meson lifetime", ICHEP-96 PA1-041, Paper Contributed to the XXVIII International Conference on High Energy Physics, 25-31 July 96, Warsaw, Poland.

[22] R.Akers et al., OPAL Collab., Z. Phys. **C67** (1995) 379

[23] SLD Collab., "Measurement of the B^+ and B^0 Lifetimes from Semileptonic Decays at SLD", ICHEP-96 PA05-084, Paper Contributed to the XXVIII International Conference on High Energy Physics, 25-31 July 96, Warsaw, Poland.

[24] SLD Collab., "Measurement of the B^+ and B^0 Lifetimes with topological vertexing at SLD", ICHEP-96 PA05-085, Paper Contributed to the XXVIII International Conference on High Energy Physics, 25-31 July 96, Warsaw, Poland.

[25] Albajar *et al.*, UA1 Collab. *Phys. Lett.* B **273**, 540 (1991).

[26] D. Buskulic et al., ALEPH Collab., CERN-PPE/96-30, Phys. Lett. **B**

[27] D. Buskulic et al., ALEPH Collab., CERN-PPE/95-92, Submitted to Z. Phys. **C**

[28] CDF Collab.,"Measurement of the Lifetime of the B_s^0 Meson from $D_s\ell$ Correlation", ICHEP-96 PA05-098d, Paper Contributed to the XXVIII International Conference on High Energy Physics, 25-31 July 96, Warsaw, Poland

[29] F. Abe et al., CDF Collab., FERMILAB-PUB-96/101 E, Submitted to Phys. Rev. Lett.

[30] DELPHI Collab.,"Mean lifetime of the B_s^0 meson", ICHEP-96 PA01-042, Paper Contributed to the XXVIII International Conference on High Energy Physics, 25-31 July 96, Warsaw, Poland

[31] P. Abreu et al., DELPHI Collab., CERN-PPE/96-32, Submitted to Z. Phys.

[32] R.Akers et al., OPAL Collab., Phys. Lett. **B350** (1995) 273

[33] ALEPH Collab.,"Updated Measurement of the b Baryon Lifetime", ICHEP-96 PA01-068, Paper Contributed to the XXVIII International Conference on High Energy Physics, 25-31 July 96, Warsaw, Poland.

[34] D. Buskulic et al., ALEPH Collab.,CERN-PPE/96-081, Submitted to Phys. Lett. **B**

[35] F. Abe et al., CDF Collab.,FERMILAB-PUB-96/089-E, Submitted to Phys. Rev. Lett.

[36] P. Abreu et al., DELPHI Collab., CERN–PPE/96–21, Submitted to Z. Phys.

[37] P. Abreu et al., DELPHI Collab., Z. Phys. **C68** (1995) 375

[38] P. Abreu et al., DELPHI Collab., Z. Phys. **C68** (1995) 541

[39] R.Akers et al., OPAL Collab., Z. Phys. **C69** (1996) 195

[40] R.Akers et al., OPAL Collab., Phys. Lett. **B353** (1995) 402

[41] D. Busculic *et al.*, ALEPH Collab., *Phys. Lett.* B **311**, 425 (1993).

[42] P. Abreu *et al.*, DELPHI Collab., *Phys. Lett.* B **324**, 500 (1994).

[43] P.D.Acton *et al.*, OPAL Collab., *Phys. Lett.* B **337**, 196 (1994).

[44] D. Busculic *et al.*, ALEPH Collab., *Phys. Lett.* B **380**, 442 (1996).

[45] P. Abreu *et al.*, DELPHI Collab., *Phys. Lett.* B **324**, 500 (1994).

[46] ALEPH Collab., "Search for the Bc meson in hadronic Z decays", ICHEP-96 PA01-069, Paper Contributed to the XXVIII International Conference on High Energy Physics, 25-31 July 96, Warsaw, Poland.

[47] M. Gronau, A. Nippe and J.L Rosner, Phys. Rev. **D 47** (1993) 1988.

[48] E.J. Eichten, C.T. Hill and C. Quigg, Phys. Rev. Lett. **71** (1993) 4116.

[49] D. Busculic *et al.*, ALEPH Collab., *Phys. Lett.* B **313**, 535 (1993).

[50] P. Abreu *et al.*, DELPHI Collab., "Inclusive Measurement of the b-quark fragmentation function", ICHEP-96 PA01-024, Paper Contributed to the XXVIII International Conference on High Energy Physics, 25-31 July 96, Warsaw, Poland.

[51] O. Adriani *et al.*, L3 Collab., *Phys. Lett.* B **345**, 589 (1995).

[52] D. Busculic *et al.*, ALEPH Collab., *Z. Phys.* C **69**, 393 (1996).

[53] P. Abreu *et al.*, DELPHI Collab., CERN-PPE/95-53, submitted to Zeit. f. Physik C.

[54] D. Busculic *et al.*, ALEPH Collab., "Resonant Structure and Flavour-tagging in the $B\pi$ System Using Fully Reconstructed B Decays", ICHEP-96 PA01-70, Paper Contributed to the XXVIII International Conference on High Energy Physics, 25-31 July 96, Warsaw, Poland.

[55] P.D.Acton *et al.*, OPAL Collab., *Z. Phys.* C **66**, 19 (1995).

[56] P. Abreu *et al.*, DELPHI Collab., *Phys. Lett.* B **345**, 598 (1995).

[57] P. Abreu *et al.*, DELPHI Collab., "Observation of Orbitally Excited B and B_s Mesons", ICHEP-96 PA01-19, Paper Contributed to the XXVIII International Conference on High Energy Physics, 25-31 July 96, Warsaw, Poland.

[58] P. Abreu *et al.*, DELPHI Collab., First Evidence for Σ_b and Σ_b^* Baryons", ICHEP-96 PA01-25, Paper Contributed to the XXVIII International Conference on High Energy Physics, 25-31 July 96, Warsaw, Poland.

[59] For a review see: P.J. Franzini, Phys. Rep. **173** (1989) 1.

[60] A. Ali and D. London, "CP Violation and Flavour Mixing in the Standard Model-1996 Update", DESY 96-140, presented at the QCD Euroconference 96, Montpellier.

[61] H. Albrecht *et al.*, ARGUS Collab., *Phys. Lett.* B **192**, 245 (1987).

[62] R. Aleksan, "CP Violation and $B^0 - \bar{B}^0$ mixing, Proceedings of the International Europhysics Conference on High Energy Physics, 27 Jul - 2 Aug 1995, Brussels, Belgium.

[63] D. Busculic *et al.*, ALEPH Collab., CERN-PPE/96-102.

[64] P. Abreu *et al.*, DELPHI Collab., "Measurement of $B_d^0 - \bar{B}_d^0$ oscillations", ICHEP-96 PA1-038, Paper Contributed to the XXVIII International Conference on High Energy Physics, 25-31 July 96, Warsaw, Poland.

[65] P.D.Acton *et al.*, OPAL Collab., CERN-PPE/96-074.

[66] P.D.Acton *et al.*, OPAL Collab., *Z. Phys.* C **66**, 543 (1995).

[67] P.D.Acton *et al.*, OPAL Collab., "A study of B Meson Oscillations using Inclusive Lepton Events", ICHEP-96 PA8-011, Paper Contributed to the XXVIII International Conference on High Energy Physics, 25-31 July 96, Warsaw, Poland.

[68] O. Adriani *et al.*, L3 Collab., CERN-PPE/96-73.

[69] D. Busculic *et al.*, ALEPH Collab., *Phys. Lett.* B **361**, 221 (1995).

[70] D. Busculic *et al.*, ALEPH Collab., *Phys. Lett.* B **311**, 425 (1993).

[71] D. Busculic *et al.*, ALEPH Collab., CERN–PPE/96–30.

[72] S. Emery, private communication.

[73] D. Busculic *et al.*, ALEPH Collab., "Search for B_s oscillations using inclusive D_s events", ICHEP-96 PA05-054, Paper Contributed to the XXVIII International Conference on High Energy Physics, 25-31 July 96, Warsaw, Poland.

[74] P. Abreu *et al.*, DELPHI Collab., "Search for $B_s^0 - \bar{B}_s^0$ oscillations", ICHEP-96 PA1-039, Paper Contributed to the XXVIII International Conference on High Energy Physics, 25-31 July 96, Warsaw, Poland.

[75] H. Moser, "Parameters for mixing analysis", ALEPH internal note, ALEPH 96-009.

[76] D. Busculic *et al.*, ALEPH Collab., "Combined limit on B_s^0 oscillations", ICHEP-96 PA08-020, Paper Contributed to the XXVIII International Conference on High Energy Physics, 25-31 July 96, Warsaw, Poland.

[77] P. Coyle, "B mixing at LEP" in Proceedings of the XI topical workshop on $p\bar{p}$ collider physics, Abano Terme (Padova), Italy, May 26 th - June 1st.

Druck: Dokumentationsstelle des Max-Planck-Instituts für extraterrestrische Physik, 85740 Garching